

RSC Advances



This is an *Accepted Manuscript*, which has been through the Royal Society of Chemistry peer review process and has been accepted for publication.

Accepted Manuscripts are published online shortly after acceptance, before technical editing, formatting and proof reading. Using this free service, authors can make their results available to the community, in citable form, before we publish the edited article. This *Accepted Manuscript* will be replaced by the edited, formatted and paginated article as soon as this is available.

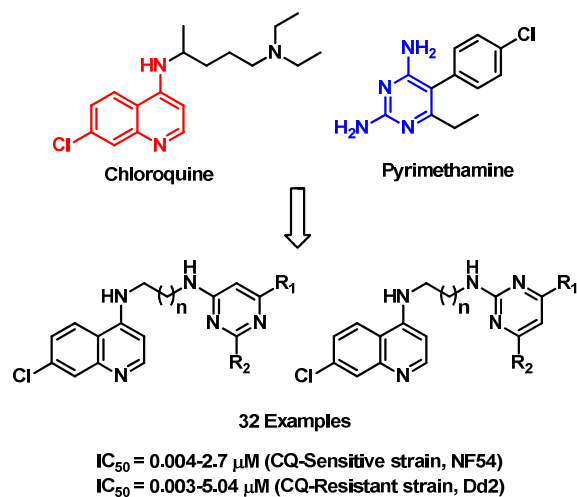
You can find more information about *Accepted Manuscripts* in the [Information for Authors](#).

Please note that technical editing may introduce minor changes to the text and/or graphics, which may alter content. The journal's standard [Terms & Conditions](#) and the [Ethical guidelines](#) still apply. In no event shall the Royal Society of Chemistry be held responsible for any errors or omissions in this *Accepted Manuscript* or any consequences arising from the use of any information it contains.

Highly active 4-aminoquinoline-pyrimidine based molecular hybrids as potential next generation antimalarial agents

Sunny Manohar, V. Satya Pavan, Dale Taylor, Deepak Kumar, Prija Ponnann, Lubbe Wiesner and Diwan S. Rawat

Novel 4-aminoquinoline-pyrimidine based antimalarial hybrids were discovered to show potent activity against NF54 and Dd2 strains of *P. falciparum*.



Cite this: DOI: 10.1039/c0xx00000x

www.rsc.org/xxxxxx

ARTICLE TYPE

Highly active 4-aminoquinoline-pyrimidine based molecular hybrids as potential next generation antimalarial agents

Sunny Manohar,^{a#} V. Satya Pavan,^a Dale Taylor,^b Deepak Kumar,^a Prija Ponnann,^a Lubbe Wiesner^b and Diwan S. Rawat^{*a}

Received (in XXX, XXX) Xth XXXXXXXXX 20XX, Accepted Xth XXXXXXXXX 20XX
DOI: 10.1039/b000000x

In order to overcome the problem of emerging drug resistance in malarial chemotherapy, a series of highly active 4-aminoquinoline-pyrimidine hybrids were synthesized and evaluated for their antimalarial activity against CQ-sensitive (NF54) and CQ-resistant (Dd2) strains of *P. falciparum* in an *in-vitro* assay. The most active hybrid **19f** exhibited 74-fold better potency than chloroquine and 4-fold better potency than artesunate against drug-resistant strain of *P. falciparum*. Compound **19e**, when evaluated for *in vivo* activity in *P. berghei*-mouse malaria model showed 93.9% parasite suppression at 30 mg/kg dose on day 4 with mean survival time of 11 days. To gain insights towards mechanism of action of these hybrids, heme binding and molecular modelling studies were performed on the most active hybrids. It was observed that inhibition of formation of β -hematin and dihydrofolate reductase-thymidylate synthase (PfDHFR-TS) enzyme could be associated with the observed antimalarial activity of these compounds.

Introduction

In recent times, the emergence of drug resistance is one of the worst nightmares to tackle in the present scenario of malaria related public health programs. The severity of this problem is indicated in the WHO recent report, which revealed an estimated 207 million cases of malaria in 2012 with an approximately 627,000 deaths. Out of these deaths, 482,000 deaths were of children under the age of five.¹ The statistics of this level are highly alarming and a message for the entire world to devote considerable efforts towards this problem. The *P. falciparum*, *P. vivax*, *P. ovale* and *P. malariae* *P. knowlesi* are the main causative species of malaria but *P. falciparum* is the most virulent species of the malaria parasite causing most of the malaria related deaths in humans.² The traditional first line antimalarial drugs such as quinine (1), chloroquine (CQ, 2) and amodiaquine (3) (figure 1) considered as a mainstay for antimalarial chemotherapy for a long period of time have lost their efficacy and their usage as antimalarial drugs has been limited due to the ever increasing *P. falciparum* drug resistance.³ According to the WHO,¹ currently the only best available treatment, particularly for *P. falciparum* related uncomplicated and severe malarial infection is artemisinin-based double- or triple-combination therapies (ACTs) where the core compound artemisinin (4) or its derivatives [dihydroartemisinin (5)/artemether (6)/arteether (7)] (figure 1) is administered in combination with locally active partner drug [piperazine (8)/pyrimethamine (9)/ sulfadoxine (10)/lumefantrine (11)/ mefloquine (12)] (figure 1). However, recent reports on the development of resistance towards artemisinin in some south-east Asian countries including Cambodia, Myanmar, Thailand and Vietnam¹ has again propelled the dire need of novel next generation antimalarials having a

broad spectrum of antimalarial activity and such compounds should be robust enough to reduce the evolution of new resistance for a longer period of time. The multi-targeting approaches based on combination therapies such as ACTs suffers from several chemicals, therapeutic and treatment related limitations.⁴ In addition, a greater precision is required for the fine-tuning of the formulation in combination therapies as the chemical species involved have different solubility's and pharmacokinetic properties.

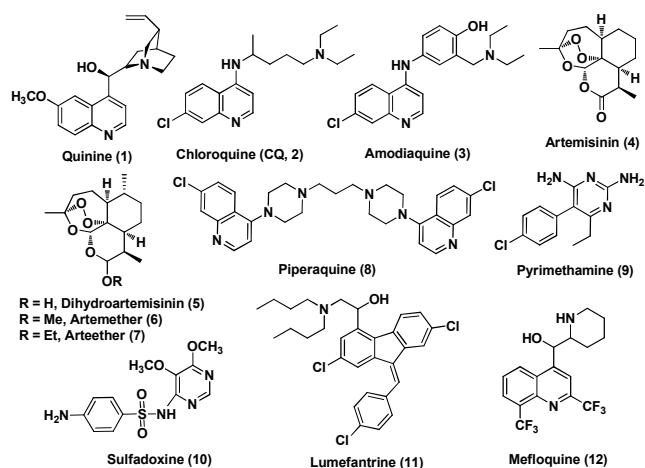


Fig. 1: Antimalarial drugs

To overcome these challenges, a better and rational alternative is to gain therapeutic benefits by developing single multi-targeted hybrid by covalent hybridization of two or more differential target-selective antimalarial entities.⁵ These dual-drug kinds of hybrids have the potential to increase bio-pharmaceutical

efficacy, reduce cost, decreases risk of drug-drug interactions and overcome rapid development of resistance problems. Various research groups across the world have successfully employed this hybridization approach towards the synthesis of interesting hybrids which have the potential of eliminating drug resistance.⁶

Our lab has successfully adopted this covalent bi-therapy strategy to generate hybrid antimalarials in which 4-aminoquinoline entity derived from CQ was covalently attached to pharmacophoric framework present in antifolate class of antimalarial drugs such as cycloguanil/pyrimethamine.⁷⁻⁹ The hybrids were designed in such a way that quinoline part of CQ is retained, in order to retain its hemozoin inhibition ability while the side chain of CQ was modified by conjugating it with triazine/pyrimidine moieties which can inhibit plasmodial DHFR and at the same time not be recognized by drug effluxing proteins. The rationality behind choosing 4-aminoquinoline skeleton, despite growing evidences of the skeleton becoming ineffective due to resistance, is based on its brilliant features like excellent clinical efficacy, ease of administration, low toxicity and cheap synthesis which makes the pharmacophore very difficult to abandon. Moreover, the hybridization strategy has the potential to restore the efficacy of traditional 4-aminoquinoline drugs such as CQ. So, the conceptual idea was to develop 4-aminoquinoline based multi-actionable architectures having dual functionality of inhibiting two conventional targets (hemozoin and plasmodial DHFR) simultaneously and in-turn could bring an upsurge of antimalarial activity particularly against resistant strains of *P. falciparum*. In our previous report,^{8,9} we have identified two highly active 4-aminoquinoline-pyrimidine hybrids (**13** and **14**; figure 2a) as lead compounds having potent *in-vitro* antimalarial activity against both CQ-sensitive (D6 clone) and CQ-resistant (W2 clone) of *P. falciparum* with no cytotoxicity against mammalian cells. The hybrids also possessed excellent *in-vivo* antimalarial activity when tested in *P. berghei* infected mouse malaria model. This level of activity warrants their selection as a potential drug candidate for preclinical trials. An in-depth analysis of antimalarial activity pattern reported for this series of 4-aminoquinoline-pyrimidine hybrids revealed three important points which are kept in mind while synthesizing new hybrid molecules (figure 2b). These are: 1) lengthening and shortening of carbon spacer linker does not play an important role in influencing antimalarial activity when Cl is substituted with amino functionalities; 2) The activity increases manifold when Cl is replaced with amino functionalities (morpholine, piperidine, *N*-methyl piperidine and *N*-ethyl piperazine); 3) The comparison of antimalarial activity of two groups of regioisomers clearly indicated that both the regioisomers displayed more or less similar potency against both the strains of *P. falciparum*. This shows that the point of attachment of the spacer to the pyrimidine nucleus may not have a great impact on antimalarial activity profile. During the progress of this work, Singh *et al*¹⁰ also reported antimalarial activity of 4-aminoquinoline-pyrimidine hybrids against Dd2 and D10 strains of *P. falciparum* with high selectivity indices and inferior toxicity when tested *in-vitro*. However, they did not carry out *in vivo* antimalarial activity of these hybrids.

Encouraged by these results and as a part of our on-going work towards the synthesis of novel antimalarial agents,^{7-9,11} we got

interested to generate a new series of 4-aminoquinoline-pyrimidine hybrids, so as to present their elaborated structure activity relationship (SAR) and to recognize novel molecular leads for finding alternative next generation antimalarial drugs. In the present investigation, we report herein new pyrimidine tethered 4-aminoquinoline based molecular hybrids synthesized by systematic chemical modification of previous lead molecules and to evaluate their antimalarial activity against both CQ-sensitive and resistant strains of *P. falciparum in vitro* and against *P. berghei* mouse malaria model *in-vivo*.

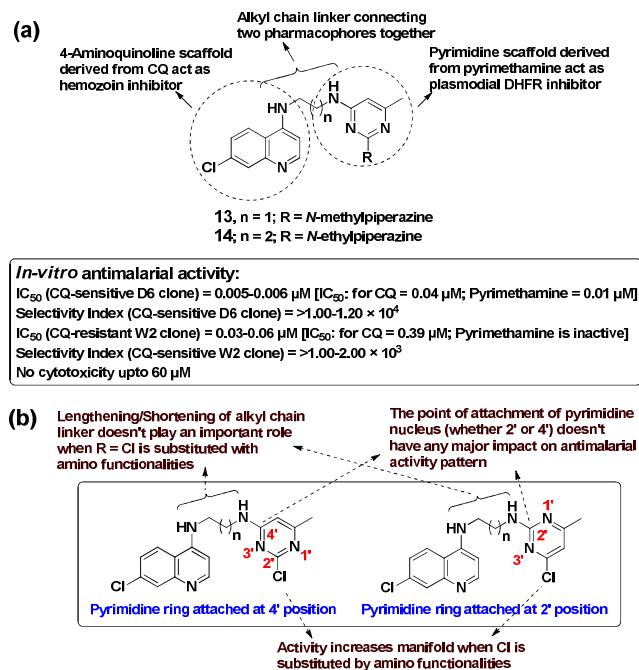
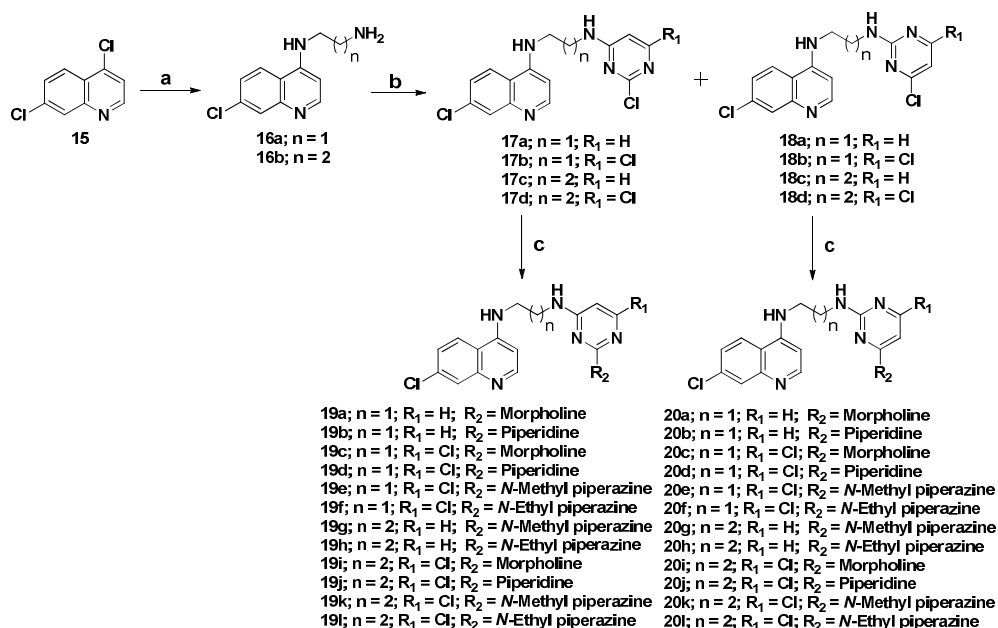


Fig. 2: a) 4-Aminoquinoline-pyrimidine hybrids (**13** and **14**) identified as lead candidates from our earlier studies.^{8,9} b) Useful structural features as determined by SAR studies on our previously reported 4-aminoquinoline-pyrimidine hybrids.

Results and discussion

Chemistry

In order to gain insights towards the determination of structural features required for displaying potent antimalarial activity and keeping the above mentioned SAR studies in mind, a series of thirty two 4-aminoquinoline-pyrimidine hybrids (**17a-17d**, **18a-18d**, **19a-19l**, **20a-20l**) were prepared by taking same amino functionalities, but altering the carbon spacer from C2 to C3 only. Additionally, the methyl group attached to pyrimidine nucleus is replaced by H and Cl, so as to see its effect on antimalarial activity pattern. The synthesis of these hybrids took place following a three step procedure reported by our lab previously.^{8,9} In short, commercially available starting material 4,7-dichloroquinoline (**15**) was taken and converted to substituted 4-aminoquinolines (**16a** and **16b**) by treatment with an excess of aliphatic linear chain diaminoalkanes having 2-3 carbon spacer via a S_NAr reaction under neat conditions. The free terminal amino groups of the substituted 4-aminoquinolines (**16a** and **16b**) were then reacted with substituted pyrimidines to yield a set of two regioisomeric intermediates (**17a-17d** and **18a-18d**) differing in the position of attachment of the pyrimidine nucleus to the



Scheme 1: a) Diaminoalkanes (n = 1-2), neat, 120-130 °C, 6-8 h, 80-90%; b) 2,4-dichloropyrimidine or 2,4,6-trichloropyrimidine, TEA, EtOH, RT, 10-12 h; c) secondary amines, DMF, 100-120 °C, 10-12 h, 50-85%.

alkyl chain linker. The intermediates (**17a-17d** and **18a-18d**) were finally converted to the targeted 4-aminoquinoline-pyrimidine hybrids (**19a-19l** and **20a-20l**) in moderate to excellent yield by treatment with various cyclic secondary amines (scheme 1).

Antimalarial Activity and Cytotoxicity

In the present investigation, we also determined antimalarial activity of two previously identified lead molecules (**13** and **14**)⁸ for the validation and comparison purpose and to check their potency against CQ-sensitive (NF54) and CQ-resistant (Dd2) strains of *P. falciparum*. Most of the hybrids showed potent antimalarial activity against both the strains of *P. falciparum*. Out of thirty two synthesized hybrids, nineteen hybrids (**18d**, **19a-19f**, **19i**, **19k**, **19l**, **20a**, **20b**, **20d-20f**, and **20i-20l**) with IC₅₀ values ranging from 0.003-0.198 μM, displayed superior activity than CQ (IC₅₀ = 0.222 μM), while four hybrids (**19f**, **19l**, **20e** and **20f**) with IC₅₀ values ranging from 0.003-0.011 μM exhibited superior activity than artesunate (IC₅₀ = 0.013 μM) when tested against CQ-resistant (Dd2 clone) strain of *P. falciparum*. Moreover, six hybrids (**19a**, **19b**, **20b**, **20f**, **20k** and **20l**) with IC₅₀ values ranging from 0.009-0.025 μM also exhibited enhanced activity than CQ (IC₅₀ = 0.027 μM) when tested against CQ-sensitive (NF54 clone) strain of *P. falciparum*. The lead molecules (**13** and **14**) from our previously published results also showed an equal level of potency against both the strains in the present investigation. Increasing the length of the linker that connects 4-aminoquinoline to pyrimidine by one carbon seems to significantly increase activity (hybrid **17a** vs **17c**, **17b** vs **17d**, **18a** vs **18c** and **18b** vs **18d**); however, this does not appear to be an important factor if the secondary cyclic amine is attached to pyrimidine (for example if we move from hybrid **19c** to **19i** or **20c** to **20i**, activity increases whereas moving from hybrid **19e** to **19k** or **19f** to **19l** activity drops with increase in carbon chain

linker). Additionally, the presence of a second Cl atom at the pyrimidine appears to be critical for determining antimalarial activity against CQ-resistant strains (hybrid **17a/18a** vs **17b/18b** and hybrid **17d/18d** vs **17c/18c**). The noticeable lack of activity with hybrid **17a/18a** may well be a combination of the shortened linking chain and the single Cl in the pyrimidine ring. The two sets of regio-isomers (hybrids **17a-17d** vs **18a-18d** and hybrids **19a-19l** vs **20a-20l**) were mostly potent to same extent which is in accordance with our earlier observation that point of attachment of pyrimidine nucleus to 4-aminoquinoline scaffold via carbon spacer linker doesn't have any major impact on determining antimalarial activity pattern. Ethyl/methyl piperazines as amino functionalities in the pyrimidine nucleus generally bring an upsurge of antimalarial activity when compared to morpholine/piperidine counterparts. The most active hybrid of the present series was found to be hybrid **19f** (IC₅₀ value 0.003 μM against CQ-resistant and IC₅₀ value 0.028 μM against CQ-sensitive strain of *P. falciparum*) with C2 carbon spacer linker attached at one of the position while Cl and ethyl piperazine as the other two groups attached to pyrimidine nucleus. SAR studies further revealed that, when a methyl group attached to pyrimidine nucleus was replaced with H or Cl, activity was retained against drug-resistant *P. falciparum* strains, but dropped slightly against drug-sensitive *P. falciparum* strains. This observation showed that methyl group is essential for imparting improved antimalarial activity against CQ-sensitive strain of *P. falciparum*.

One of the highly active hybrids, **19e** was further evaluated for the *in-vivo* antimalarial activity against *P. berghei* infected mice (table 2 and figure 3) and it was found out that it causes 93.9 % parasite suppression at 30 mg/kg dose on day 4 with mean survival time being 11 days post-infection. In comparison, CQ showed 90.3 % suppression at 15 mg/kg dose. The parasite suppression data was calculated by the formula given below.

$$\text{Parasite suppression\%} = [1 - (\text{group parasitemia} / \text{placebo parasitemia})] \times 100$$

1) For the tested hybrids, cytotoxicity appeared at much higher concentrations than the concentrations responsible for their antimalarial activity indicating compounds safe toxicity profile. The most toxic of the hybrids was found to be compound **20j** with IC₅₀ value 11.09 μM while the least toxic is hybrid **20i** (IC₅₀ value is 230.77 μM). The high selectivity index (the ratio of IC₅₀ for cytotoxicity to CHO cells and IC₅₀ for antimalarial activity against CQ-resistant strains revealing an estimate of a therapeutic window) for most of the hybrids further revealed their potency against the tested *Plasmodium* isolates. Three hybrids (**19f**, **19k** and **19l**) showed selectivity index > 5000 whereas other displayed in the range of 220 to 4347. Five hybrids (**19a**, **19f**, **19k**, **19l** and **20f**) were found to have greater selectivity index (in the range of 4070-10758) than the previously identified lead molecules **13** and **14**. To know the probable mode of action of these hybrids, heme binding and molecular modelling studies were further performed on the most active hybrid.

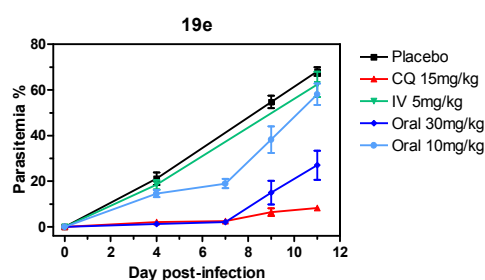


Fig. 3: Parasite levels in mice infected with *Plasmodium berghei* ANKA and treated orally or intravenously with compound **19e** for 4 consecutive days. The data represent mean ± SEM.

Heme Binding Studies

Chloroquine and other 4-aminoquinoline derivatives are believed to show their antimalarial action by interfering with the parasite feeding process during which heme ferriprotoporphyrin-IX is generated which is very toxic to the parasite but through a unique mechanism, parasite detoxifies it within the food vacuole by crystallizing it to insoluble granules of non-toxic material called hemozoin. Hemozoin is an insoluble ionic polymer in which adjacent heme units are linked *via* a carboxylate iron (III) coordinate bond. Hemozoin was originally considered to be formed by the polymerization of heme, but it has now been demonstrated to be a crystalline cyclic dimer of ferriprotoporphyrin-IX.¹² It is widely accepted that CQ accumulates in the plasmodium food vacuole and inhibit the process of formation of hemozoin, by forming a complex with heme/hematin which in turn leaves heme in an uncrystallised form which has a toxic effect and eventually kills the parasite. Cohen *et al* were the first to show that CQ forms a complex with ferriprotoporphyrin-IX (FPIX) in aqueous solution, which was proved by the changes in the UV-spectrum of aqueous hematin in the presence of drug.¹³ Later on, several studies explained the formation of CQ-hematin complex by computational methods as well as the spectroscopic methods.¹⁴ More recently it has been determined that CQ forms complexes with both monomeric and μ-oxo dimeric FPIX.¹⁵ Therefore, we decided to evaluate the binding of the one of the most active compound **19f** from the series with heme.

A solution of hematin in 40% DMSO showed a Soret band at 402 nm, indicating the presence of monomeric heme under the conditions used (0.02 M HEPES buffer, pH 7.4 and 0.02 M MES buffer, pH 5.6). The stepwise addition of small increments of compound **19f** into a constant concentration of monomeric heme (5.0 μM) resulted in a substantial decrease in the intensity of the Fe(III) PPIX Soret band at 402 nm with no shift in the absorption maximum. This indicates the association of compounds with hematin (figure 4). Solvent (DMSO) did not affect the binding of compound **19f** with heme at the pH values used in this experiment. The stoichiometry ratio of the most stable complexes of compound **19f** with monomeric heme at pH 7.5 and 5.6 was deduced from the Job's plot. The absorbance at 402 nm got to maximum when the mole fraction of the compound was approximately 0.5. Thus 1:1 ratio was established for the association of compound heme at both the pH values (figure 5).

As discussed earlier that CQ and its derivatives also bind to heme dimer (μ-oxo heme). Therefore, the binding of compound **19f** was also studied with μ-oxo dimers of heme at pH 5.8. A solution of heme in aqueous NaOH showed a peak at 362 nm. Addition of compound **19f** (0-20 μM) to a solution of μ-oxo dimer (10 μM) in 20 mM phosphate buffer at pH 5.8 resulted in a decrease in intensity of absorbance at 362 nm (figure 6A), which shows the interaction between heme and the compound **19f**. The Job's plot indicated a 1:1 stoichiometry for the most stable μ-oxo heme:compound **19f** complex (figure 6B). The association constants for the complexes formed between monomeric Fe (III) PPIX and compound **19f** at pH 7.4 and 5.6 were calculated by the analysis of titration data and are presented in Table 3.

Table 3: Binding constants for compound **19f** and chloroquine with heme.

Compound	Monomeric heme log K (pH = 7.4)	Monomeric heme log K (pH = 5.6)	μ-oxo-heme log K (pH = 5.8)
19f	5.19	5.81	5.83
CQ	5.15 ¹⁰	4.65 ¹⁰	5.58 ¹⁰
Stoichiometry	1:1	1:1	1:1

The association constants for the complexes formed between monomeric heme and compound **19f** at pH 7.5 (log K 5.19) were found to be almost equivalent to the standard antimalarial drug CQ (log K 5.15).¹⁰ Furthermore, decreasing the pH from 7.4 to 5.6 (food vacuole pH), compound has shown improved binding constant (log K 5.81) indicating that binding is stronger even at acidic pH of food vacuole. Interestingly, compound **19f** showed the larger value of the binding constant than the standard drug chloroquine at pH 5.6. The association constants for the binding with μ-oxo heme at pH 5.8 (log K 5.83) was found to be even greater than the monomeric heme complexes. From the data shown in table 3, it is clear that the compound **19f** binds strongly with monomeric heme (log K 4.63) as well as μ-oxo-heme (log K 5.83) and the observed results are comparable to the standard CQ (log K 5.58). Thus the formation of a complex between heme and compound **19f** suggests the inhibition of formation of β-hematin, which could be correlated to the observed antimalarial activity of these compounds in a fashion similar to that of CQ.

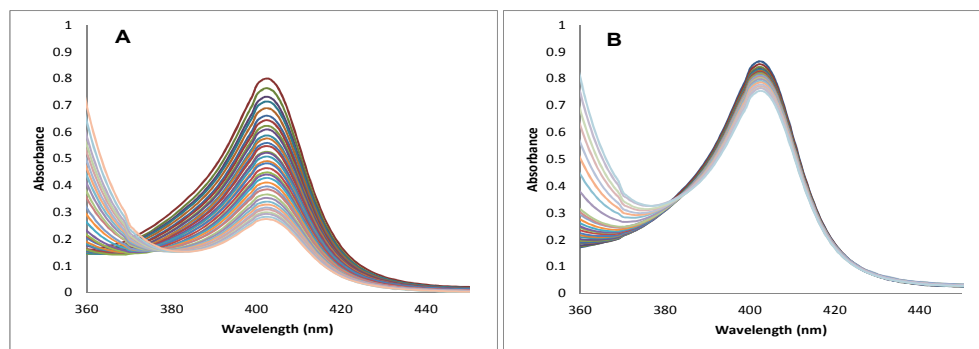


Fig. 4: A) Titration of compound **19f** with monomeric heme at pH 7.5; B) Titration of compound **19f** with monomeric heme at pH 5.6

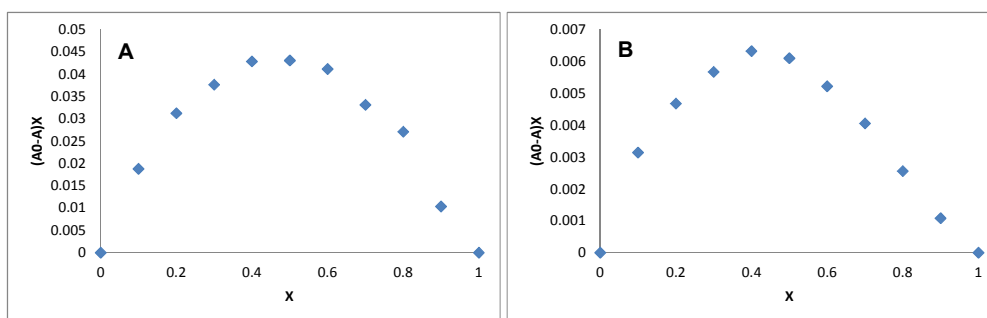


Fig. 5: Job's plot of monomeric heme complex formation with compound **19f**; A) at pH 7.4; B) at pH 5.6; X (mole fraction of the compound **19f**) = [compound **19f**]/[compound **19f**] + [heme]; A0 is the absorbance, when x = 1 and A is the absorbance at respective values of x

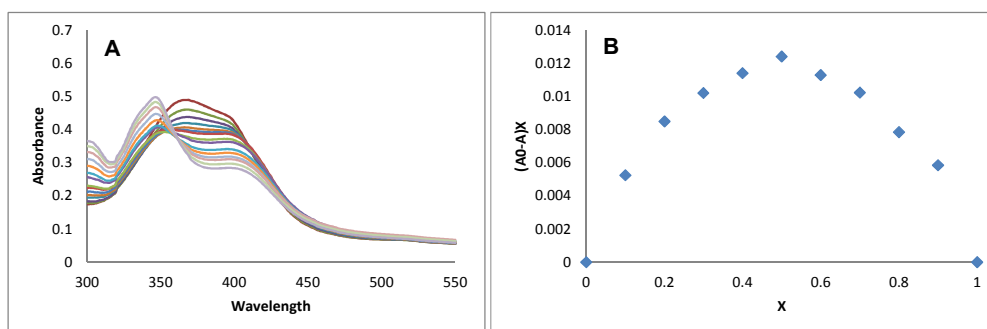


Fig. 6: A) Titration of compound **19f** with μ -oxo dimeric heme at pH 5.8; B) Job's plot of μ -oxo dimeric heme complex formation with compound **19f** at pH 5.8.

Molecular Modelling studies

a) Binding mode analysis

With the emergence of resistance to most of the antimalarial drugs especially quinoline and antifolate class of drugs, the quest for novel drug candidate for malaria is needed. Antifolates act by inhibiting dihydrofolate reductase activity of *Plasmodium falciparum* bifunctional enzyme dihydrofolate reductase-thymidylate synthase (*Pf*-DHFR-TS). Occurrence of four point mutations in codons 51, 59, 108, and 164 (N51I, C59R, S108N and I164L) in the DHFR domain of *Pf*-DHFR-LS gene from the clinical isolates of dihydrofolate resistant parasite shed light on

the cause of dihydrofolate resistance.¹⁶ In the present work we have attempted to study the interactions of novel 4-aminoquinoline-pyrimidine based hybrid compounds with *Pf*-DHFR-TS.

For this purpose molecular docking studies of best active compounds (**19a**, **19e**, **19f**, **19l**, **20b**, **20e**, **20f**) were performed in the binding pocket of both the wild type *Pf*-DHFR-TS (PDB ID:3QGT) and quadruple mutant *Pf*-DHFR-TS (N51I, C59R, S108 N, I164L, PDB ID:3QG2) structures. The results of docking studies and the docked conformations of best scored ligands (**19a** and **20e**) in the active site of wild and mutant *Pf*-DHFR-TS are illustrated in table 4 and figures 6 and 7. These docking results clearly indicate that the most active compounds in the study exhibited significant binding affinities towards the wild (Glide energy range -51.64 kcalmol⁻¹ to -40.52 kcalmol⁻¹) and quadruple

mutant (Glide energy range -54.09 kcalmol $^{-1}$ to -42.81 kcalmol $^{-1}$) *Pf*-DHFR-TS structures and the energy ranges are comparable to that of reference compounds (pyrimethamine, cycloguanil and WR99210) and the native substrate of DHFR dihydrofolate (Table 4).

The compounds showed hydrogen bond interactions along with π - π interactions in the predicted binding poses. Compound **20e** showing lowest binding energy (-54.09 kcalmol $^{-1}$) and considerable high Glide score (-8.18 kcalmol $^{-1}$) for mutant *Pf*-DHFR with formation of hydrogen bonds between a linker NH group of compound **20e** and oxygen side chain of Asp54 of both wild and mutant *Pf*-DHFR. Further π - π interactions between aromatic ring of Phe58 and 4-chloropyrimidine ring of compound are observed (figure 7). An additional H-bond between main chain oxygen atom of Ser111 and quinolone nitrogen was observed in the docking mode of wild *Pf*-DHFR. Another

compound predicted to have low binding energy (-42.55 Kcalmol $^{-1}$) and high glide score (-7.09) was compound **19a**, showing similar H-bond pattern between linker NH group of compound and oxygen side chain of Asp54. The π - π interactions between aromatic ring of Phe58 and 4-chloropyrimidine ring of compound were also observed (figure 8). No H-bond was observed between the compound and Ser111 of the proteins. The influence of quadruple mutations in DHFR (N51I, C59R, S108 N, I164L) is attributed to the movement of the active site residues and interferes in the inhibitor binding. N51I causes movement in main chain atoms of residues 48-51 and C59R mutation does not cause any significant changes in the protein structure. Residues 51 and 59 lie in the proximity of the active site residue Asp54, which has been reported crucial for inhibitors and substrate binding.

Table 4: Glide docking scores (kcal mol $^{-1}$) and docking energies of best active molecules along with the reference compounds (Pyrimethamine, cycloguanil and WR99210) and dihydrofolate bound to wild and mutant *Pf*DHFR-TS binding site

Comp	Docking results with wild <i>Pf</i> DHFR				Docking results with mutant <i>Pf</i> DHFR			
	Glide Score	Glide lipo	Glide H-bond	Glide Energy	Glide Score	Glide lipo	Glide H-bond	Glide Energy
19a	-7.09	-3.05	-0.19	-42.55	-7.37	-3.29	-0.35	-51.07
19e	-5.63	-2.82	-0.18	-40.52	-7.17	-1.95	-0.17	-44.48
19f	-5.88	-2.87	-0.26	-43.55	-5.36	-1.78	-0.21	-42.81
19l	-6.40	-3.27	-0.22	-44.23	-6.28	-3.73	-0.46	-46.77
20b	-6.97	-3.14	0.25	-51.64	-6.31	-3.51	-0.32	-48.93
20e	-8.21	-2.83	-0.32	-51.20	-8.18	-3.20	-0.42	-54.09
20f	-6.44	-2.29	-0.27	-41.80	-6.56	-4.47	-0.45	-43.8
Dihydrofolate	-9.34	-2.27	-0.72	-44.85	-8.88	-2.37	-0.74	-59.48
Pyrimethamine	-8.82	-2.55	-0.85	-65.11	-9.39	-3.01	-0.82	-32.48
Cycloguanil	-8.77	-1.89	-0.88	-57.97	-9.28	-2.43	-0.73	-39.05
WR99210	-5.61	-2.0	0.52	-39.04	-7.61	-2.51	-0.30	-40.08

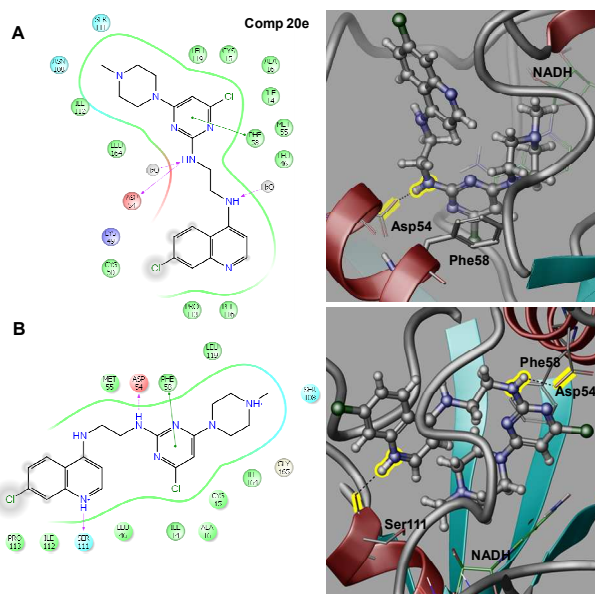


Fig. 7: 2D and 3D docking pose showing interaction for compound **20e** in the binding site of (A) mutant *Pf*DHFR-TS (PDB ID: 3QG2); (B) wild *Pf*-DHFR-TS (PDB ID: 3QGT)

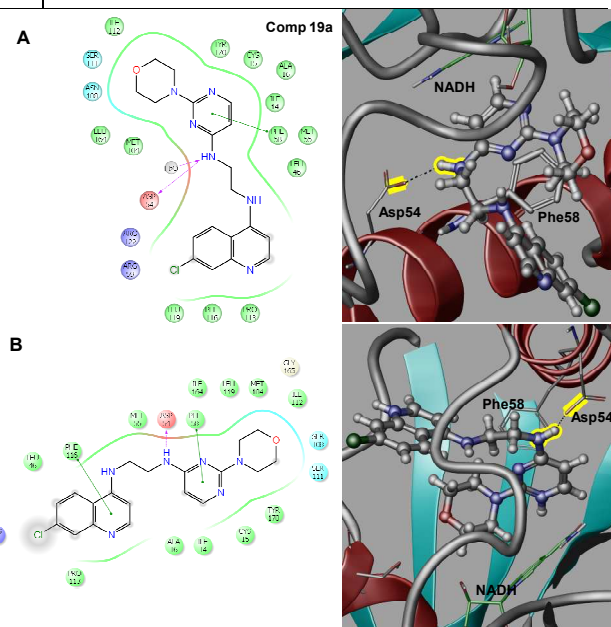


Fig. 8: 2D and 3D docking pose showing interaction for compound **19a** in the binding site of (A) mutant *Pf*DHFR-TS (PDB ID: 3QG2); (B) wild *Pf*-DHFR-TS (PDB ID: 3QGT).

In the present docking study, we have observed H-bond interactions of test compound with Asp54 similar to the DHFR native substrate dihydrofolate. Moreover, the function of Asp54 residue is preserved in the mutant protein and not affected by the two proximal mutations N51I and C59R.¹⁷ Further, I164L mutation causes shifts in the residues 164-167 and affects the gap in the active site causing steric interactions of Phe58 with small inhibitors such as pyrimethamine and cycloguanil. The test compounds form a long distance interaction with Phe58 forming π - π interaction, thus avoiding steric clash with the aromatic side chain of Phe58. In *Pf*-DHFR S108N mutation, the *p*-chlorophenyl moiety in pyrimethamine and cycloguanil cause steric interference with the side chain of Asn108 in the modified active site. Thus, it becomes appropriate to explore the binding pattern of novel lead compound in the preliminary stages of drug design against mutant proteins. Figure 9 shows the binding mode of test compounds used in the study in comparison with the *Pf*-DHFR inhibitors (Pyrimethamine, Cycloguanil and WR99210) in the active site of the mutant *Pf*-DHFR structure. In S108N mutation, the *p*-chlorophenyl moiety in pyrimethamine and cycloguanil cause steric interference with the side chain of Asn108 in the modified active site mutant *Pf*-DHFR. Whereas, WR99210 having flexible linker does not show steric hindrance with Asn108. It was observed that WR99210 occupies similar surface volume as the *Pf*-DHFR native substrate (dihydrofolate). Several observations have shown that drug molecules designed to occupy the surface volume of the native substrate of the protein will be less susceptible to resistance occurring due to steric clashes in the mutated protein binding site.¹⁸ Hence, we have performed molecular overlay of docking poses of active test compounds along *Pf*-DHFR inhibitors (Pyrimethamine, Cycloguanil and WR99210) on the dihydrofolate surface envelope and it is clear from the figure 9 that the test compounds occupy the similar volume as that of the protein substrate unlike Pyrimethamine and Cycloguanil to avoid the steric clash with the side chain of Asn108.

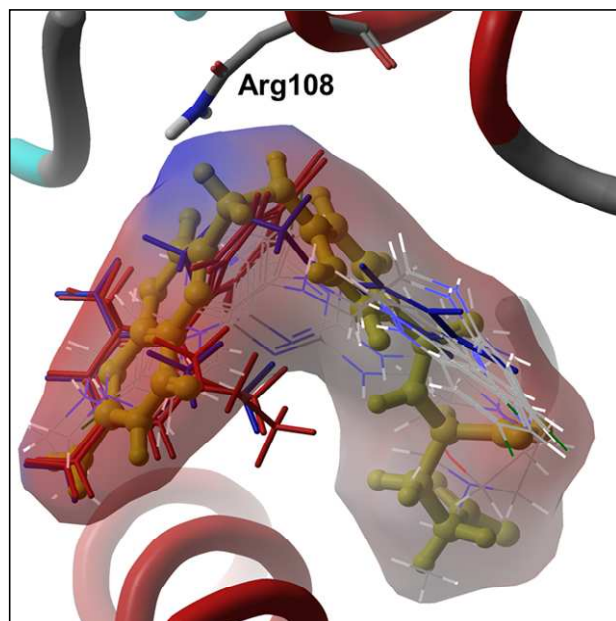


Fig. 9: Molecular overlay of most active docked test compounds (represented as wireframe format with atom colours), Pyrimethamine (red

sticks), Cycloguanil (red sticks), WR99210 (blue sticks) and the *Pf*-DHFR substrate dihydrofolate (yellow ball and stick) bound to the binding site of quadruple mutant *Pf*-DHFR (PDB ID: 3QG2) showing the fitting of the test compounds and the *Pf*-DHFR inhibitors in the surface area occupied by the *Pf*-DHFR substrate (dihydrofolate).

b) Prediction of Pharmacokinetic Properties

Different pharmacokinetic parameters of compounds in the study, showing good inhibitory potential in malarial parasites were calculated using ADMET predictions by Qikprop.¹⁹ The most important of these parameters together with its permissible ranges are listed in the table 5 and 6. As a preliminary test of the drug-likeness of the compounds, we calculated Lipinski's rule of 5 using QikProp (table 5). An orally active compound should not have more than four violations of these rules. In the present study, all the active compounds showed "0" value for Lipinski's rule of 5 violations, indicating that these active test compounds have good drug likeness properties similar to the reference molecules pyrimethamine and cycloguanil.

Prediction of oral drug absorption (Percent Human Oral Absorption) was highly satisfactory for all the test compounds. Studies have suggested that oral bioavailability is influenced by compound's flexibility and can be measured by the number of rotatable bonds (<15) and polar surface area (70 \AA^2 - 200 \AA^2).²⁰ In the present study, all the test compounds have a number of rotatable bonds <15 and polar surface area falls satisfactorily in the permissible range (table 6). Similarly, molecules following Lipinski's rule of 5 are more likely to have good intestinal absorption or permeation which is confirmed by the predicted Caco-2 cells permeability (QPPCaco), used as a model for the gut-blood barrier.²¹ QPPCaco predictions for all the test compounds showed very good values with the exception for compound **19e** having slightly good values for Caco-2 cells permeability and is comparable to the value predicted for the drug pyrimethamine. Further, QPlogK_{hsa}, the prediction for human serum albumin binding and all inhibitors were predicted to lie within the expected range for 95% of known drugs (-1.5 to 1.5). Also, the QikProp descriptor for brain/blood partition coefficient (QPlogBB) and the blood-brain barrier mimic MDCK cell permeability (QPPMDCK) show satisfactory predictions for all the test compounds and the reference compounds.

80

Table 5: Prediction of Lipinski's 'Rule of 5' for the active test compounds^a

Comp	mol_M W (> 500)	donor rHB (<5)	accept HB (<10)	QPlog Po/w (<5)	Rule of Five (<4)
19a	384.86	2	7	3.74	0
19e	432.35	2	7	4.11	0
19f	446.38	2	7	4.61	0
19l	460.40	2	7	4.9	0
20b	382.89	2	5	4.72	0
20e	432.35	2	7	4.1	0
20f	446.38	2	7	4.47	0
Pyrimethamine	248.7	4	3	1.81	0
Cycloguanil	253.73	5	3	0.89	0

^a All values calculated by QikProp v 3.5 and the explanations of the descriptors are given in the text

Table 6: Calculated ADMET properties

Compound	Percent Human Oral Absorption (>80% high, <25% poor) ^a	QPPCaco nms ⁻¹ (<25 poor, >500 great) ^a	QPlogBB (-3.0-1.2) ^a	QPPMDCK (<25 poor; >500 great) ^a	QPlogKhsa (-1.5 to 1.5) ^a	PSA (7.0-200.0) ^a	#rotor (0-15) ^a
19a	100	2159.46	-0.26	2084.40	0.24	68.4	5
19e	100	497.61	0.22	1479.7	0.529	64.08	5
19f	100	564.96	0.21	1714.28	0.611	68.75	6
19i	100	596.79	0.14	1967.53	0.75	63.43	7
20b	100	2432.89	-0.23	3190.13	0.65	56.91	5
20e	100	584.59	0.27	1556.19	0.51	61.93	5
20f	100	632.19	0.23	1693.53	0.611	61.42	6
Pyrimethamine	84.34	412.28	-0.78	468.85	-0.24	73.73	4
Cycloguanil	68.8	111.854	-0.17	126.64	-0.30	76.36	2

^aCalculated using QikProp v 3.5. Range/recommended values calculated for 95% known drugs

Conclusions

In conclusion, a series of thirty two highly active 4-aminoquinoline-pyrimidine hybrids were synthesised using a three step procedure and evaluated for their antimalarial activity against both CQ-sensitive and CQ-resistant strains of *P. falciparum*. 19 hybrids (18d, 19a-19f, 19i, 19k, 19l, 20a, 20b, 20d-20f, and 20i-20l) displayed superior antimalarial activity than CQ while 4 hybrids (19f, 19l, 20e and 20f) exhibited better antimalarial activity than artesunate against drug-resistant *P. falciparum* strain. The most active hybrid 19f showed 74-fold better activity than CQ and around 4-fold better activity than artesunate in the assay. Inhibition of formation of β -hematin and dihydrofolate reductase-thymidylate synthase (*Pf*-DHFR-TS) enzyme could be associated to the observed antimalarial activity of these compounds as observed by heme binding and molecular modelling studies. Compounds 19a and 20e were predicted to show good binding with wild type and mutant *Pf*-DHFR proteins with interaction pattern comparable to that of DHFR inhibitors and native DHFR substrate. Moreover, the test compounds efficiently bind with the mutant protein avoiding steric clashes resulting from the amino acid mutations. The calculated *in silico* ADMET parameters for all the active test compounds indicated good drug likeness character and pharmacokinetic properties, making them important candidates in the anti-malarial drug discovery process. This level of activity coupled with their possible mechanism of action of inhibiting two targets simultaneously within a system permits their further investigation as a lead candidate in malarial chemotherapy for the production of next generation antimalarials.

Acknowledgements

DSR thank University of Delhi and DU-DST PURSE for financial support. SM and DK are thankful to CSIR for the award of junior and senior research fellowship. SPV is thankful to UGC for junior research fellowship [File No: 41-20282012(SR)]. PP is thankful to CSIR for Research Associate. DT and LW are thankful to South African National Research Foundation for funding support. The authors are also thankful to CIF-USIC, University of Delhi, Delhi for NMR & HRMS data.

Experimental Section

Instrumentation and chemicals

All of the chemicals used in the synthesis were purchased from Sigma-Aldrich and were used as such. Thin layer chromatography was used to monitor the progress of the reactions and checked by pre-coated TLC plates (E. Merck Kieselgel 60 F₂₅₄) with spots being visualized by iodine vapors. Compounds were purified over silica gel (60-120 mesh) column or recrystallized with suitable solvents. Solvents were distilled before using for purification purposes. Melting points were recorded on an ERS automated melting point apparatus and are uncorrected. IR spectra were recorded using Perkin-Elmer Bruker FT-IR and the values are expressed as λ_{\max} cm⁻¹. HRMS data were recorded on Agilent G6530 AA LC-HRMSQ-TOF instrument. The ¹H NMR and ¹³C NMR spectra were recorded on Jeol Spectrospin spectrometer at 400 MHz and 100 MHz respectively. The referencing was done using TMS as an internal standard in case of CDCl₃ solvent and with residual DMSO peak in case of DMSO-*d*₆ solvent. The chemical shift values are recorded on δ scale and the coupling constants (*J*) are in Hz.

General procedure for the synthesis of compounds 16a-b

A mixture of 4,7-dichloroquinoline (1 eq.) and diaminoalkane (5 eq.) was heated at 120-130 °C under nitrogen atmosphere for 6-8 h. Ice was added to the reaction mixture and reaction mixture was stirred at 0 °C for 1 h. The precipitate thus formed was filtered, washed with cold water (100 mL) and dried. The crude product was dissolved in 50 ml CHCl₃ and washed with water (3 × 250 mL) and finally with brine. Organic layer was dried over Na₂SO₄ and excess of solvent was removed under vacuum. The crude product thus obtained was recrystallized by CHCl₃/hexane system to get pale yellow solid of compound 16a and 16b.

N1-(7-Chloroquinolin-4-yl)ethane-1,2-diamine (16a)²²: Yield: 90%; mp 139-141 °C; ¹H NMR (400 MHz, DMSO-*d*₆) 2.86 (t, *J* = 6.0 Hz, 2 H, CH₂); 3.27-3.29 (m, 2 H, CH₂); 4.53 (brs, 2 H, NH₂); 6.47 (d, *J* = 5.3 Hz, 1 H, ArH); 7.37-7.42 (m, 2 H, NH and ArH); 7.75 (d, *J* = 2.2 Hz, 1 H); 8.26-8.29 (m, 1 H, ArH); 8.37 (d, *J* = 5.3 Hz, 1 H, ArH); HRMS (ESI, *m/z*) calcd for C₁₁H₁₃ClN₃:

222.0793 (MH)⁺; Found: 222.0796.

***N*¹-(7-Chloroquinolin-4-yl)propane-1,3-diamine (16b)**²²: Yield: 80%; mp 95-97 °C; ¹H NMR (400 MHz, DMSO-*d*₆) 1.73-1.76 (m, 2 H, CH₂); 2.71 (t, *J* = 6.0 Hz, 2 H, CH₂); 3.29-3.32 (m, 2 H, CH₂); 4.04 (brs, 2 H, NH₂); 6.45 (d, *J* = 5.3 Hz, 1 H, ArH); 7.40-7.42 (m, 2 H, NH and ArH); 7.75 (d, *J* = 2.2 Hz, 1 H); 8.22-8.25 (m, 1 H, ArH); 8.35-8.37 (m, 1 H, ArH); HRMS (ESI, *m/z*) calcd for C₁₂H₁₅ClN₃: 236.0949 (MH)⁺; Found: 236.0946.

General procedure for the synthesis of compounds 17a-d and 18a-d

To a well stirred solution of 2,4-dichloropyrimidine or 2,4,6-trichloropyrimidine (1 eq.) and triethylamine (2 eq.) in ethanol (50 ml) at room temperature was added diamines (1 eq.). The reaction mixture was allowed to stir overnight at room temperature. After completion of reaction as evident by TLC, reaction mixture was poured into ice cold water (250 ml) and precipitate thus formed was filtered and washed with excess of water at vacuum pump. The crude precipitate was dissolved in 100 ml of CHCl₃ and extracted with water (2 × 500 ml) and finally with brine. Excess of solvent was evaporated to dryness under vacuum and the crude product thus obtained was purified by SiO₂ column using MeOH/CHCl₃ as eluent to yield respective compounds **17a-d** and **18a-d**.

***N*¹-(2-chloropyrimidin-4-yl)-*N*²-(7-chloroquinolin-4-yl)ethane-1,2-diamine (17a)**: Yield: 65%; mp 234-236 °C; IR (cm⁻¹, KBr): 3253, 2967, 1608, 1585, 1427, 1237, 1142, 901, 792; ¹H NMR (400 MHz, DMSO-*d*₆): 3.42-3.46 (m, 4 H, CH₂); 6.62-6.75 (m, 2 H, ArH); 7.45 (dd, *J* = 8.7 Hz, 2.2 Hz, 1 H, ArH); 7.53 (brs, 1 H, NH); 7.78-7.79 (m, 2 H); 8.20 (d, *J* = 8.7 Hz, 1 H, ArH); 8.28 (brs, 1 H, NH); 8.40 (d, *J* = 5.1 Hz, 1 H, ArH); ¹³C NMR (100 MHz, DMSO-*d*₆): 41.5, 98.8, 109.2, 117.3, 124.1, 124.3, 126.9, 133.7, 148.3, 150.5, 151.3, 159.9, 160.1, 162.3; HRMS (ESI, *m/z*) calcd for C₁₅H₁₄Cl₂N₅: 334.0621 (MH)⁺; Found: 334.0627; Anal. Calcd for C₁₅H₁₃Cl₂N₅: C, 53.91; H, 3.92; N, 20.96; Found: C, 53.73; H, 3.98; N, 21.03.

***N*¹-(7-chloroquinolin-4-yl)-*N*²-(2,6-dichloropyrimidin-4-yl)ethane-1,2-diamine (17b)**: Yield: 68%; mp 237-239 °C; IR (cm⁻¹, KBr): 3266, 3113, 1610, 1572, 1449, 1239, 1099, 811, 794; ¹H NMR (400 MHz, DMSO-*d*₆): 3.44-3.50 (m, 4 H, CH₂); 6.69 (d, *J* = 5.1 Hz, 1 H, ArH); 6.88 (s, 1 H); 7.42-7.45 (m, 2 H, NH and ArH); 7.77 (d, *J* = 2.2 Hz, 1 H, ArH); 8.18 (d, *J* = 9.5 Hz, 1 H, ArH); 8.27 (brs, 1 H, NH); 8.40 (d, *J* = 5.1 Hz, 1 H, ArH); ¹³C NMR (100 MHz, DMSO-*d*₆): 41.1, 98.7, 107.7, 117.4, 123.9, 124.1, 127.3, 133.4, 148.8, 150.1, 151.6, 160.8, 161.1, 161.5; HRMS (ESI, *m/z*) calcd for C₁₅H₁₃Cl₃N₅: 368.0231 (MH)⁺; Found: 368.0235; Anal. Calcd for C₁₅H₁₂Cl₃N₅: C, 48.87; H, 3.28; N, 19.00; Found: C, 48.96; H, 3.45; N, 18.82.

***N*¹-(2-chloropyrimidin-4-yl)-*N*³-(7-chloroquinolin-4-yl)propane-1,3-diamine (17c)**: Yield: 60%; mp 185-187 °C; IR (cm⁻¹, KBr): 3264, 2956, 1596, 1430, 1364, 1165, 1093, 787; ¹H NMR (400 MHz, DMSO-*d*₆): 1.87-1.92 (m, 2 H, CH₂); 3.30-3.35 (m, 4 H, CH₂); 6.46 (d, *J* = 5.8 Hz, 1 H, ArH); 6.63 (d, *J* = 5.1 Hz, 1 H,

ArH); 7.32 (brs, 1 H, NH); 7.43 (dd, *J* = 8.7 Hz, 2.2 Hz, 1 H, ArH); 7.75-7.77 (m, 2 H, NH and ArH); 8.19-8.25 (m, 2 H, ArH); 8.36 (d, *J* = 5.1 Hz, 1 H, ArH); ¹³C NMR (100 MHz, DMSO-*d*₆): 28.1, 39.5, 99.5, 109.6, 118.3, 124.9, 128.1, 134.2, 149.7, 150.9, 152.5, 160.7, 163.1; HRMS (ESI, *m/z*) calcd for C₁₆H₁₆Cl₂N₅: 348.0777 (MH)⁺; Found: 348.0782; ESI-MS (*m/z*): 348.13, 350.13 (MH + 2)⁺; Anal. Calcd for C₁₆H₁₅Cl₂N₅: C, 55.19; H, 4.34; N, 20.11; Found: C, 55.25; H, 4.49; N, 20.01.

***N*¹-(7-chloroquinolin-4-yl)-*N*³-(2,6-dichloropyrimidin-4-yl)propane-1,3-diamine (17d)**: Yield: 55%; mp 205-207 °C; IR (cm⁻¹, KBr): 3259, 3116, 2937, 1609, 1590, 1457, 1141, 1092, 861, 794; ¹H NMR (400 MHz, DMSO-*d*₆): 1.87-1.93 (m, 2 H, CH₂); 3.31-3.37 (m, 4 H, CH₂); 6.44-6.45 (m, 1 H, ArH); 6.81-6.84 (m, 1 H, ArH); 7.28 (brs, 1 H, NH); 7.42 (dd, *J* = 8.7 Hz, 2.2 Hz, 1 H, ArH); 7.76 (d, *J* = 2.2 Hz, 1 H, ArH); 8.22-8.24 (m, 2 H, NH and ArH); 8.36 (d, *J* = 5.1 Hz, 1 H, ArH); ¹³C NMR (100 MHz, DMSO-*d*₆): 27.5, 39.4, 99.3, 107.9, 118.0, 124.65, 124.68, 128.1, 133.9, 149.6, 150.6, 152.4, 161.3, 161.7, 162.0; HRMS (ESI, *m/z*) calcd for C₁₆H₁₅Cl₃N₅: 382.0387 (MH)⁺; Found: 382.0384; Anal. Calcd for C₁₆H₁₄Cl₃N₅: C, 50.22; H, 3.69; N, 18.30; Found: C, 50.12; H, 3.60; N, 18.43.

***N*¹-(4-chloropyrimidin-2-yl)-*N*²-(7-chloroquinolin-4-yl)ethane-1,2-diamine (18a)**: Yield: 30%; mp 216-218 °C; IR (cm⁻¹, KBr): 2427, 1600, 1431, 1384, 1242, 978, 763; ¹H NMR (400 MHz, DMSO-*d*₆): 3.50-3.52 (m, 4 H, CH₂); 6.44 (d, *J* = 5.8 Hz, 1 H, ArH); 6.79 (d, *J* = 5.8 Hz, 1 H, ArH); 7.48 (dd, *J* = 8.7 Hz, 2.2 Hz, 1 H, ArH); 7.82 (d, *J* = 2.2 Hz, 1 H, ArH); 7.86 (d, *J* = 5.8 Hz, 1 H, ArH); 8.19 (brs, 1 H, NH); 8.30 (brs, 1 H, NH); 8.34 (d, *J* = 8.7 Hz, 1 H, ArH); 8.40 (d, *J* = 5.8 Hz, 1 H, ArH); ¹³C NMR (100 MHz, DMSO-*d*₆): 38.2, 41.3, 98.8, 105.2, 116.8, 124.7, 124.9, 134.8, 145.6, 148.9, 151.9, 155.6, 159.8, 163.5; HRMS (ESI, *m/z*) calcd for C₁₅H₁₄Cl₂N₅: 334.0621 (MH)⁺; Found: 334.0625; Anal. Calcd for C₁₅H₁₃Cl₂N₅: C, 53.91; H, 3.92; N, 20.96; Found: C, 53.99; H, 3.76; N, 20.88.

***N*¹-(7-chloroquinolin-4-yl)-*N*²-(4,6-dichloropyrimidin-2-yl)ethane-1,2-diamine (18b)**: Yield: 28%; mp 235-237 °C; IR (cm⁻¹, KBr): 3352, 2944, 2860, 1612, 1568, 1451, 1366, 1272, 1173, 985, 829, 764; ¹H NMR (400 MHz, DMSO-*d*₆): 3.47-3.57 (m, 4 H, CH₂); 6.53 (s, 1 H, ArH); 6.71 (d, *J* = 5.1 Hz, 1 H, ArH); 7.46 (d, *J* = 8.8 Hz, 1 H, ArH); 7.58 (brs, 1 H, NH); 7.78 (d, *J* = 2.2 Hz, 1 H, ArH); 8.21 (d, *J* = 8.8 Hz, 1 H, ArH); 8.41-8.42 (m, 2 H); ¹³C NMR (100 MHz, DMSO-*d*₆): 41.7, 99.5, 103.5, 117.9, 124.7, 124.9, 127.4, 134.4, 148.8, 151.0, 151.8, 157.5, 159.6, 164.9; HRMS (ESI, *m/z*) calcd for C₁₅H₁₃Cl₃N₅: 368.0231 (MH)⁺; Found: 368.0228; Anal. Calcd for C₁₅H₁₂Cl₃N₅: C, 48.87; H, 3.28; N, 19.00; Found: C, 48.95; H, 3.44; N, 19.13.

***N*¹-(4-chloropyrimidin-2-yl)-*N*³-(7-chloroquinolin-4-yl)propane-1,3-diamine (18c)**: Yield: 35%; mp 234-236 °C; IR (cm⁻¹, KBr): 3255, 2964, 2920, 1597, 1463, 1431, 1343, 1083, 977, 765; ¹H NMR (400 MHz, DMSO-*d*₆): 1.90-1.94 (m, 2 H, CH₂); 3.30-3.35 (m, 4 H, CH₂); 6.44-6.48 (m, 2 H, ArH); 7.35 (brs, 1 H, NH); 7.44 (dd, *J* = 8.7 Hz, 2.2 Hz, 1 H, ArH); 7.78 (d, *J* = 2.2 Hz, 1 H, ArH); 7.87 (d, *J* = 5.8 Hz, 1 H, ArH); 8.00 (brs, 1 H, NH); 8.27 (d, *J* = 8.7 Hz, 1 H, ArH); 8.38 (d, *J* = 5.1 Hz, 1 H, ArH); ¹³C

NMR (100 MHz, DMSO-*d*₆): 27.0, 37.9, 98.7, 105.1, 117.4, 124.1, 127.3, 133.5, 148.8, 150.1, 151.7, 155.3, 159.9, 163.4; HRMS (ESI, *m/z*) calcd for C₁₆H₁₆Cl₂N₅: 348.0777 (MH)⁺; Found: 348.0783; Anal. Calcd for C₁₆H₁₅Cl₂N₅: C, 55.19; H, 4.34; N, 20.11; Found: C, 55.13; H, 4.41; N, 20.24.

***N*¹-(7-chloroquinolin-4-yl)-*N*³-(4,6-dichloropyrimidin-2-yl)propane-1,3-diamine (18d)**: Yield: 35%; mp 195-198 °C; IR (cm⁻¹, KBr): 3266, 3141, 2870, 1578, 1450, 1118, 973, 826, 796; ¹H NMR (400 MHz, DMSO-*d*₆): 1.89-1.93 (m, 2 H, CH₂); 3.28-3.32 (m, 4 H, CH₂), 6.45-6.48 (m, 2 H, ArH); 7.29 (brs, 1 H, NH); 7.42 (dd, *J* = 8.8 Hz, 2.2 Hz, 1 H, ArH); 7.77 (d, *J* = 2.2 Hz, 1 H, ArH); 8.23-8.25 (m, 2 H, NH and ArH), 8.37 (d, *J* = 5.8 Hz, 1 H, ArH); ¹³C NMR (100 MHz, DMSO-*d*₆): 26.9, 38.4, 98.7, 102.7, 117.4, 124.0, 127.3, 133.4, 148.9, 150.0, 151.7, 156.6, 159.0, 164.1; HRMS (ESI, *m/z*) calcd for C₁₆H₁₅Cl₃N₅: 382.0388 (MH)⁺; Found: 382.0385; Anal. Calcd for C₁₆H₁₄Cl₃N₅: C, 50.22; H, 3.69; N, 18.30; Found: C, 50.27; H, 3.75; N, 18.40.

General procedure for the synthesis of compounds 19a-1

In a 100 mL round bottom flask, compound 17a-d (1 eq.) was taken and dissolved in 10 mL of DMF. To this, a solution of respective amine (3 eq.) in DMF (5 ml) was added dropwise. Reaction mixture was allowed to stir at 100-120 °C for 10 h monitored by TLC (scheme 1.5). After completion, water (50 ml) was added to reaction mixture and it was extracted with EtOAc (2 × 25 mL). Organic layer was then collected, washed with water (2 × 100 mL) and brine, dried over Na₂SO₄ and finally excess of solvent was evaporated under vacuum. The crude residue thus obtained was purified by SiO₂ column using MeOH/CHCl₃ as eluent to afford compounds 19a-1.

***N*¹-(7-chloroquinolin-4-yl)-*N*²-(2-morpholinopyrimidin-4-yl)ethane-1,2-diamine (19a)**: Yield: 66%; mp 128-130 °C; IR (cm⁻¹, KBr): 3248, 2969, 1585, 1481, 1240, 1116, 976, 793; ¹H NMR (400 MHz, DMSO-*d*₆): 3.37-3.51 (m, 8 H, CH₂); 3.56-3.58 (m, 4 H); 6.00 (d, *J* = 5.1 Hz, 1 H, ArH); 6.53 (d, *J* = 5.1 Hz, 1 H, ArH); 6.72 (brs, 1 H, NH); 7.40-7.42 (m, 2 H, NH and ArH); 7.74 (d, *J* = 2.2 Hz, 1 H, ArH); 7.84 (s, 1 H, ArH); 8.13 (d, *J* = 8.7 Hz, 1 H, ArH); 8.34 (d, *J* = 5.8 Hz, 1 H, ArH); ¹³C NMR (100 MHz, DMSO-*d*₆): 42.7, 43.6, 65.8, 93.1, 98.6, 117.4, 123.8, 124.1, 127.5, 133.3, 149.0, 150.1, 151.9, 156.7, 161.9, 162.4; HRMS (ESI, *m/z*) calcd for C₁₉H₂₂ClN₆O: 385.1537 (MH)⁺; Found: 385.1542; Anal. Calcd for C₁₉H₂₁ClN₆O: C, 59.29; H, 5.50; N, 21.84; Found: C, 59.18; H, 5.35; N, 21.92.

***N*¹-(7-chloroquinolin-4-yl)-*N*²-(2-(piperidin-1-yl)pyrimidin-4-yl)ethane-1,2-diamine (19b)**: Yield: 72%; mp 147-149 °C; IR (cm⁻¹, KBr): 3386, 2940, 2853, 1565, 1584, 1365, 1236, 1128, 978, 792; ¹H NMR (400 MHz, DMSO-*d*₆): 1.42-1.55 (m, 6 H, CH₂); 3.43-3.48 (m, 8 H, CH₂); 5.99 (d, *J* = 5.1 Hz, 1 H, ArH); 6.52 (d, *J* = 5.8 Hz, 1 H, ArH); 6.62 (brs, 1 H, NH); 7.40 (dd, *J* = 8.7 Hz, 2.2 Hz, 1 H, ArH); 7.46 (brs, 1 H, NH); 7.74 (d, *J* = 2.2 Hz, 1 H, ArH); 7.78 (s, 1 H, ArH); 8.12 (d, *J* = 8.7 Hz, 1 H, ArH); 8.34 (d, *J* = 5.8 Hz, 1 H, ArH); ¹³C NMR (100 MHz, DMSO-*d*₆): 24.2, 25.1, 44.2, 93.2, 98.6, 117.3, 123.8, 124.1, 127.4, 133.3, 149.0, 150.1, 151.8, 156.3, 161.8, 162.0; HRMS

(ESI, *m/z*) calcd for C₂₀H₂₄ClN₆: 383.1745 (MH)⁺; Found: 383.1745; Anal. Calcd for C₂₀H₂₃ClN₆: C, 62.74; H, 6.05; N, 21.95; Found: C, 62.88; H, 6.15; N, 22.10.

***N*¹-(6-chloro-2-morpholinopyrimidin-4-yl)-*N*²-(7-chloroquinolin-4-yl)ethane-1,2-diamine (19c)**: Yield: 80%; mp 148-150 °C; IR (cm⁻¹, KBr): 3378, 2971, 2853, 1580, 1516, 1369, 1331, 1248, 1121, 974, 784; ¹H NMR (400 MHz, CDCl₃): 3.44-3.48 (m, 2 H, CH₂); 3.54-3.56 (m, 4 H, CH₂), 3.70-3.73 (m, 4 H, CH₂), 3.82-3.88 (m, 2 H, CH₂), 5.47 (brs, 1 H, NH); 5.99 (s, 1 H, ArH); 6.33 (d, *J* = 5.1 Hz, 1 H, ArH); 6.87 (brs, 1 H, NH); 7.31 (d, *J* = 8.0 Hz, 1 H, ArH); 7.80-7.92 (m, 2 H, ArH); 8.48 (d, *J* = 5.1 Hz, 1 H, ArH); ¹³C NMR (100 MHz, DMSO-*d*₆): 42.1, 43.9, 65.7, 90.3, 98.6, 117.4, 123.9, 124.0, 127.5, 133.3, 149.0, 150.0, 151.8, 159.3, 161.3, 164.3; HRMS (ESI, *m/z*) calcd for C₁₉H₂₁Cl₂N₆O: 419.1148 (MH)⁺; Found: 419.1154; Anal. Calcd for C₁₉H₂₀Cl₂N₆O: C, 54.42; H, 4.81; N, 20.04; Found: C, 54.56; H, 4.98; N, 19.92.

***N*¹-(6-chloro-2-(piperidin-1-yl)pyrimidin-4-yl)-*N*²-(7-chloroquinolin-4-yl)ethane-1,2-diamine (19d)**: Yield: 75%; mp 139-141 °C; IR (cm⁻¹, KBr): 3372, 2938, 2854, 1579, 1517, 1447, 1331, 1130, 973, 784; ¹H NMR (400 MHz, DMSO-*d*₆): 1.45-1.46 (m, 4 H, CH₂); 1.57-1.58 (m, 2 H, CH₂), 3.36-3.52 (m, 8 H, CH₂), 6.05-6.15 (m, 1 H, ArH); 6.52 (d, *J* = 5.1 Hz, 1 H, ArH); 7.14 (brs, 1 H, NH); 7.38 (brs, 1 H, NH); 7.43 (dd, *J* = 8.8 Hz, 2.2 Hz, 1 H, ArH); 7.77 (d, *J* = 2.2 Hz, 1 H, ArH); 8.18 (d, *J* = 8.0 Hz, 1 H, ArH), 8.35-8.38 (m, 1 H, ArH); ¹³C NMR (100 MHz, DMSO-*d*₆): 24.4, 25.1, 43.4, 44.6, 90.0, 98.5, 117.4, 123.9, 124.0, 127.5, 133.3, 149.0, 150.0, 151.8, 159.2, 161.5, 163.9; HRMS (ESI, *m/z*) calcd for C₂₀H₂₃Cl₂N₆: 417.1355 [MH]⁺; Found 417.1350; Anal. Calcd for C₂₀H₂₂Cl₂N₆: C, 57.56; H, 5.31; N, 20.14; Found: C, 57.64; H, 5.28; N, 20.29.

***N*¹-(6-chloro-2-(4-methylpiperazin-1-yl)pyrimidin-4-yl)-*N*²-(7-chloroquinolin-4-yl)ethane-1,2-diamine (19e)**: Yield: 66%; mp 118-120 °C; IR (cm⁻¹, KBr): 3266, 2941, 2850, 1584, 1514, 1376, 1228, 1139, 971, 782; ¹H NMR (400 MHz, DMSO-*d*₆): 2.00-2.25 (m, 7 H, CH₂ and CH₃); 3.48-3.54 (m, 8 H, CH₂), 6.05-6.15 (m, 1 H, ArH); 6.51-6.75 (m, 1 H, ArH); 7.17 (brs, 1 H, NH); 7.37 (brs, 1 H, NH); 7.42 (dd, *J* = 8.8 Hz, 2.2 Hz, 1 H, ArH); 7.77 (d, *J* = 2.2 Hz, 1 H, ArH); 8.17 (d, *J* = 8.0 Hz, 1 H, ArH), 8.37 (d, *J* = 5.0 Hz, 1 H, ArH); ¹³C NMR (100 MHz, DMSO-*d*₆): 42.1, 43.5, 45.6, 54.1, 66.3, 90.3, 98.5, 117.4, 123.9, 124.1, 127.5, 133.4, 149.0, 150.1, 151.8, 159.4, 161.4, 163.0; HRMS (ESI, *m/z*) calcd for C₂₀H₂₄Cl₂N₇: 432.1465 (MH)⁺; Found: 432.1466; Anal. Calcd for C₂₀H₂₃Cl₂N₇: C, 55.56; H, 5.36; N, 22.68; Found: C, 55.71; H, 5.26; N, 22.77.

***N*¹-(6-chloro-2-(4-ethylpiperazin-1-yl)pyrimidin-4-yl)-*N*²-(7-chloroquinolin-4-yl)ethane-1,2-diamine (19f)**: Yield: 72%; mp 97-99 °C; IR (cm⁻¹, KBr): 3265, 2932, 2816, 1582, 1449, 1245, 970, 782; ¹H NMR (400 MHz, DMSO-*d*₆): 0.98 (t, *J* = 7.3 Hz, 3 H, CH₃); 2.29-2.30 (m, 6 H, CH₂); 3.44-3.49 (m, 8 H, CH₂), 6.05-6.17 (m, 1 H, ArH); 6.52-6.76 (m, 1 H, ArH); 7.19 (brs, 1 H, NH); 7.37 (brs, 1 H, NH); 7.42 (dd, *J*₁ = 8.8 Hz, 2.2 Hz, 1 H, ArH); 7.77 (d, *J* = 2.2 Hz, 1 H, ArH); 8.17 (d, *J* = 8.0 Hz, 1 H, ArH), 8.37 (d, *J* = 5.0 Hz, 1 H, ArH); HRMS (ESI, *m/z*) calcd for

$C_{21}H_{26}Cl_2N_7$: 446.1621 (MH)⁺; Found: 446.1619; Anal. Calcd for $C_{21}H_{25}Cl_2N_7$: C, 56.50; H, 5.65; N, 21.97; Found: C, 56.62; H, 5.76; N, 21.81.

***N*¹-(7-chloroquinolin-4-yl)-*N*³-(2-(4-methylpiperazin-1-yl)pyrimidin-4-yl)propane-1,3-diamine (19g)**: Yield: 61%; mp 172-175 °C; IR (cm⁻¹, KBr): 3343, 2928, 1582, 1367, 1138, 1001, 792; ¹H NMR (400 MHz, DMSO-*d*₆): 1.85-2.25 (m, 9 H, CH₂ and CH₃); 3.43-3.59 (m, 8 H, CH₂), 5.96 (s, 1 H, ArH); 6.45-6.50 (m, 1 H, ArH); 7.35-7.42 (m, 3 H, ArH and NH); 7.75-7.77 (m, 2 H, ArH); 8.23 (d, *J* = 8.7 Hz, 1 H, ArH), 8.35 (d, *J* = 5.1 Hz, 1 H, ArH); HRMS (ESI, *m/z*) calcd for $C_{21}H_{27}ClN_7$: 412.2010 (MH)⁺; Found: 412.2007; Anal. Calcd for $C_{21}H_{26}ClN_7$: C, 61.23; H, 6.36; N, 23.80; Found: C, 61.33; H, 6.38; N, 23.70.

***N*¹-(7-chloroquinolin-4-yl)-*N*³-(2-(4-ethylpiperazin-1-yl)pyrimidin-4-yl)propane-1,3-diamine (19h)**: Yield: 55%; mp 178-180 °C; IR (cm⁻¹, KBr): 3245, 2932, 1581, 1438, 1370, 1244, 1140, 974, 790; ¹H NMR (400 MHz, DMSO-*d*₆): 0.96 (t, *J* = 7.3 Hz, 3 H, CH₃); 1.84-1.86 (m, 2 H, CH₂); 2.19-2.25 (m, 6 H, CH₂); 3.31-3.38 (m, 8 H, CH₂); 5.95 (d, *J* = 5.8 Hz, 1 H, ArH); 6.43 (d, *J* = 5.8 Hz, 1 H, ArH); 6.60 (brs, 1 H, NH); 7.35 (brs, 1 H, NH); 7.43 (dd, *J* = 8.7 Hz, 2.2 Hz, 1 H, ArH); 7.74-7.76 (m, 2 H, ArH); 8.23 (d, *J* = 8.7 Hz, 1 H, ArH); 8.34 (d, *J* = 5.1 Hz, 1 H, ArH); HRMS (ESI, *m/z*) calcd for $C_{22}H_{29}ClN_7$: 426.2167 (MH)⁺; Found: 421.2160; Anal. Calcd for $C_{22}H_{28}ClN_7$: C, 62.03; H, 6.63; N, 23.02; Found: C, 62.13; H, 6.55; N, 23.16.

***N*¹-(6-chloro-2-morpholinopyrimidin-4-yl)-*N*³-(7-chloroquinolin-4-yl)propane-1,3-diamine (19i)**: Yield: 78%; mp 178-180 °C; IR (cm⁻¹, KBr): 3338, 2924, 2855, 1581, 1448, 1368, 1245, 1115, 972, 784; ¹H NMR (400 MHz, DMSO-*d*₆): 1.83-1.88 (m, 2 H, CH₂); 3.28-3.50 (m, 12 H, CH₂), 6.00 (s, 1 H, ArH); 6.44 (d, *J* = 5.1 Hz, 1 H, ArH); 7.21 (brs, 1 H, NH); 7.31 (brs, 1 H, NH); 7.42 (dd, *J* = 8.8 Hz, 2.2 Hz, 1 H, ArH); 7.75 (d, *J* = 2.2 Hz, 1 H, ArH); 8.23 (d, *J* = 8.0 Hz, 1 H, ArH), 8.35 (d, *J* = 5.0 Hz, 1 H, ArH); ¹³C NMR (100 MHz, DMSO-*d*₆): 27.5, 38.5, 43.8, 44.2, 65.6, 65.9, 89.9, 98.6, 117.4, 124.0, 127.4, 133.3, 149.0, 150.0, 151.8, 159.3, 161.2, 163.2; HRMS (ESI, *m/z*) calcd for $C_{20}H_{23}Cl_2N_6O$: 433.1305 (MH)⁺; Found: 433.1312; Anal. Calcd for $C_{20}H_{22}Cl_2N_6O$: C, 55.43; H, 5.12; N, 19.39; Found: C, 55.54; H, 5.21; N, 19.53.

***N*¹-(6-chloro-2-(piperidin-1-yl)pyrimidin-4-yl)-*N*³-(7-chloroquinolin-4-yl)propane-1,3-diamine (19j)**: Yield: 82%; mp 235-238 °C; IR (cm⁻¹, KBr): 3245, 2930, 2852, 1610, 1588, 1522, 1368, 1125, 973, 774; ¹H NMR (400 MHz, DMSO-*d*₆): 1.34-1.50 (m, 6 H); 1.80-1.85 (m, 2 H, CH₂); 3.26-3.28 (m, 4 H); 3.36-3.40 (m, 4 H, CH₂), 5.97 (s, 1 H, ArH); 6.42 (d, *J* = 5.1 Hz, 1 H, ArH); 7.06 (brs, 1 H, NH); 7.27 (brs, 1 H, NH); 7.39 (dd, *J* = 8.8 Hz, 2.2 Hz, 1 H, ArH); 7.73 (d, *J* = 2.2 Hz, 1 H, ArH); 8.20 (d, *J* = 8.0 Hz, 1 H, ArH); 8.32 (d, *J* = 5.0 Hz, 1 H, ArH); ¹³C NMR (100 MHz, DMSO-*d*₆): 24.1, 25.0, 27.5, 38.4, 44.5, 89.6, 98.6, 117.4, 124.0, 127.4, 133.3, 149.0, 150.0, 151.7, 159.2, 161.3, 162.6; HRMS (ESI, *m/z*) calcd for $C_{21}H_{25}Cl_2N_6$: 431.1512 (MH)⁺; Found: 431.1518; Anal. Calcd for $C_{21}H_{24}Cl_2N_6$: C, 58.47; H, 5.61; N, 19.48; Found: C, 58.35; H, 5.54; N, 19.32.

***N*¹-(6-chloro-2-(4-methylpiperazin-1-yl)pyrimidin-4-yl)-*N*³-(7-chloroquinolin-4-yl)propane-1,3-diamine (19k)**: Yield: 66%; mp 230-232 °C; IR (cm⁻¹, KBr): 3314, 2938, 2850, 1579, 1515, 1449, 1373, 1279, 1143, 1001, 967, 779; ¹H NMR (400 MHz, DMSO-*d*₆): 1.83-1.86 (m, 2 H, CH₂); 2.08-2.12 (m, 7 H, CH₂ and CH₃); 3.29-3.31 (m, 8 H, CH₂), 6.00 (s, 1 H, ArH); 6.44 (d, *J* = 5.1 Hz, 1 H, ArH); 7.16 (brs, 1 H, NH); 7.32 (brs, 1 H, NH); 7.43 (dd, *J* = 8.8 Hz, 2.2 Hz, 1 H, ArH); 7.76 (d, *J* = 2.2 Hz, 1 H, ArH); 8.24 (d, *J* = 8.7 Hz, 1 H, ArH), 8.35 (d, *J* = 5.8 Hz, 1 H, ArH); ¹³C NMR (100 MHz, DMSO-*d*₆): 27.5, 38.5, 43.3, 45.5, 54.0, 89.9, 98.5, 117.4, 123.9, 127.4, 133.3, 149.0, 149.9, 151.8, 159.3, 161.3, 162.9; HRMS (ESI, *m/z*) calcd for $C_{21}H_{26}Cl_2N_7$: 446.1621; Found: 446.1617; Anal. Calcd for $C_{21}H_{25}Cl_2N_7$: C, 56.50; H, 5.65; N, 21.97; Found: C, 56.51; H, 5.76; N, 21.76.

***N*¹-(6-chloro-2-(4-ethylpiperazin-1-yl)pyrimidin-4-yl)-*N*³-(7-chloroquinolin-4-yl)propane-1,3-diamine (19l)**: Yield: 58%; mp 203-205 °C; IR (cm⁻¹, KBr): 3292, 2931, 2816, 1581, 1449, 1368, 1247, 1139, 970, 853, 781; ¹H NMR (400 MHz, DMSO-*d*₆): 0.95 (t, *J* = 7.3 Hz, 3 H, CH₃); 1.83-1.86 (m, 2 H, CH₂); 2.09-2.23 (m, 6 H, CH₂); 3.29-3.37 (m, 8 H, CH₂), 5.98 (s, 1 H, ArH); 6.44 (d, *J* = 5.1 Hz, 1 H, ArH); 7.15 (brs, 1 H, NH); 7.32 (brs, 1 H, NH); 7.42 (dd, *J* = 8.8 Hz, 2.2 Hz, 1 H, ArH); 7.75 (d, *J* = 2.2 Hz, 1 H, ArH); 8.24 (d, *J* = 8.7 Hz, 1 H, ArH), 8.34 (d, *J* = 5.8 Hz, 1 H, ArH); ¹³C NMR (100 MHz, DMSO-*d*₆): 11.8, 27.6, 38.5, 43.4, 51.4, 51.8, 89.8, 98.5, 117.4, 123.9, 124.0, 127.4, 133.3, 149.0, 149.9, 151.8, 159.2, 161.3, 162.9; HRMS (ESI, *m/z*) calcd for $C_{22}H_{28}Cl_2N_7$: 406.1777 (MH)⁺; Found: 460.1783; Anal. Calcd for $C_{22}H_{27}Cl_2N_7$: C, 57.39; H, 5.91; N, 21.30; Found: C, 57.46; H, 5.96; N, 21.48.

General procedure for the synthesis of compounds 20a-l

In a 100 mL round bottom flask, compound **18a-d** (1 eq.) was taken and dissolved in 10 mL of DMF. To this, a solution of respective amine (3 eq.) in DMF (5 ml) was added drop-wise. Reaction mixture was allowed to stir at 100-120 °C for 10 h monitored by TLC. After completion, water (50 ml) was added to reaction mixture and it was extracted with EtOAc (2 × 25 mL). Organic layer was then collected, washed with water (2 × 100 mL) and brine, dried over Na₂SO₄ and finally excess of solvent was evaporated under vacuum. The crude residue thus obtained was purified by SiO₂ column using MeOH/CHCl₃ as eluent to afford compounds **20a-l**.

***N*¹-(7-chloroquinolin-4-yl)-*N*²-(4-morpholinopyrimidin-2-yl)ethane-1,2-diamine (20a)**: Yield: 85%; mp 258-260 °C; IR (cm⁻¹, KBr): 3216, 2925, 1579, 1369, 1243, 1067, 977; ¹H NMR (400 MHz, DMSO-*d*₆): 3.25-3.31 (m, 8 H, CH₂); 3.52-3.69 (m, 4 H, CH₂); 6.42 (d, *J* = 5.1 Hz, 1 H, ArH); 6.64 (d, *J* = 5.1 Hz, 1 H, ArH); 7.16 (brs, 1 H, NH); 7.34 (dd, *J* = 8.7 Hz, 2.2 Hz, 1 H, ArH); 7.80 (d, *J* = 2.2 Hz, 1 H, ArH); 7.87-7.93 (m, 2 H, ArH); 8.14 (d, *J* = 8.7 Hz, 1 H, ArH); 8.44 (d, *J* = 5.1 Hz, 1 H, ArH); HRMS (ESI, *m/z*) calcd for $C_{19}H_{22}ClN_6O$: 385.1537 (MH)⁺; Found: 385.1534; Anal. Calcd for $C_{19}H_{21}ClN_6O$: C, 59.29; H, 5.50; N, 21.84; Found: C, 59.42; H, 5.61; N, 21.92.

***N*¹-(7-chloroquinolin-4-yl)-*N*²-(4-(piperidin-1-yl)pyrimidin-2-**

yl)ethane-1,2-diamine (20b): Yield: 82%; mp 198-200 °C; IR (cm⁻¹, KBr): 3322, 2931, 2855, 1585, 1499, 1341, 1243, 796; ¹H NMR (400 MHz, DMSO-*d*₆): 1.45-1.58 (m, 6 H, CH₂); 3.42-3.52 (m, 4 H, CH₂); 3.64-3.67 (m, 4 H); 5.70 (d, *J* = 5.1 Hz, 1 H, ArH); 6.54 (d, *J* = 5.1 Hz, 1 H, ArH); 7.11 (brs, 1 H, NH); 7.42-7.44 (m, 2 H, NH and ArH); 7.69 (d, *J* = 5.1 Hz, 1 H, ArH); 7.77 (d, *J* = 2.2 Hz, 1 H, ArH); 8.17 (d, *J* = 8.7 Hz, 1 H, ArH); 8.37 (d, *J* = 5.1 Hz, 1 H, ArH); ¹³C NMR (100 MHz, DMSO-*d*₆): 24.4, 25.2, 42.1, 44.1, 95.0, 98.5, 117.4, 123.8, 123.9, 127.4, 133.3, 149.0, 150.0, 151.7, 154.9, 161.1, 162.5; HRMS (ESI, m/z) calcd for C₂₀H₂₄ClN₆: 383.1745 (MH)⁺; Found: 383.1743; Anal. Calcd for C₂₀H₂₃ClN₆: C, 62.74; H, 6.05; N, 21.95; Found: C, 62.81; H, 6.11; N, 21.96.

*N*¹-(4-chloro-6-morpholinopyrimidin-2-yl)-*N*²-(7-chloroquinolin-4-yl)ethane-1,2-diamine (20c): Yield: 80%; mp 115-117 °C; IR (cm⁻¹, KBr): 3369, 2967, 2857, 1576, 1478, 1451, 1247, 1105, 967, 783; ¹H NMR (400 MHz, DMSO-*d*₆): 3.40-3.52 (m, 12 H, CH₂); 5.77 (s, 1 H, ArH); 6.49 (d, *J* = 5.8 Hz, 1 H, ArH); 7.36 (brs, 1 H, NH); 7.40 (dd, *J* = 8.8 Hz, 2.2 Hz, 1 H, ArH); 7.48 (brs, 1 H, NH); 7.75 (d, *J* = 2.2 Hz, 1 H, ArH); 8.12 (d, *J* = 8.7 Hz, 1 H, ArH); 8.34 (d, *J* = 5.4 Hz, 1 H, ArH); ¹³C NMR (100 MHz, DMSO-*d*₆): 38.1, 41.8, 43.8, 65.9, 93.2, 98.6, 117.4, 124.0, 124.1, 127.5, 133.4, 149.1, 150.0, 151.8, 157.3, 160.8, 163.6; HRMS (ESI, m/z) calcd for C₁₉H₂₁Cl₂N₆O: 419.1148 (MH)⁺; Found: 419.1144; Anal. Calcd for C₁₉H₂₀Cl₂N₆O: C, 54.42; H, 4.81; N, 20.04; Found: C, 54.35; H, 4.90; N, 20.12.

*N*¹-(4-chloro-6-(piperidin-1-yl)pyrimidin-2-yl)-*N*²-(7-chloroquinolin-4-yl)ethane-1,2-diamine (20d): Yield: 85%; mp 201-203 °C; IR (cm⁻¹, KBr): 3327, 2932, 2850, 1578, 1486, 1329, 1286, 1142, 1064, 797; ¹H NMR (400 MHz, DMSO-*d*₆): 1.40-1.42 (m, 4 H, CH₂); 1.52-1.53 (m, 2 H, CH₂); 3.45-3.57 (m, 8 H, CH₂); 5.69 (s, 1 H, ArH); 6.49 (d, *J* = 5.1 Hz, 1 H, ArH); 7.38-7.40 (m, 3 H, NH and ArH); 7.74 (d, *J* = 2.2 Hz, 1 H, ArH); 8.12 (d, *J* = 8.7 Hz, 1 H, ArH); 8.33 (d, *J* = 5.4 Hz, 1 H, ArH); ¹³C NMR (100 MHz, DMSO-*d*₆): 24.3, 25.3, 41.9, 44.2, 66.4, 92.3, 98.6, 117.5, 124.0, 124.2, 127.5, 133.5, 149.1, 150.1, 151.8, 157.5, 160.6, 163.7; HRMS (ESI, m/z) calcd for C₂₀H₂₃Cl₂N₆: 417.1356 (MH)⁺; Found: 417.1363; Anal. Calcd for C₂₀H₂₂Cl₂N₆: C, 57.56; H, 5.31; N, 20.14; Found: C, 57.72; H, 5.48; N, 20.02.

*N*¹-(4-chloro-6-(4-methylpiperazin-1-yl)pyrimidin-2-yl)-*N*²-(7-chloroquinolin-4-yl)ethane-1,2-diamine (20e): Yield: 62%; mp 119-121 °C; IR (cm⁻¹, KBr): 3309, 2937, 2851, 1575, 1489, 1447, 1138, 1003, 943, 785; ¹H NMR (400 MHz, DMSO-*d*₆): 2.15-2.23 (m, 7 H, CH₂ and CH₃); 3.34-3.58 (m, 8 H, CH₂); 5.76 (s, 1 H, ArH); 6.51 (d, *J* = 5.8 Hz, 1 H, ArH); 7.41-7.44 (m, 2 H, NH and ArH); 7.47 (brs, 1 H, NH); 7.77 (d, *J* = 2.2 Hz, 1 H, ArH); 8.16 (d, *J* = 8.7 Hz, 1 H, ArH); 8.37 (d, *J* = 5.4 Hz, 1 H, ArH); ¹³C NMR (100 MHz, DMSO-*d*₆): 38.1, 41.8, 43.2, 45.7, 54.3, 92.8, 98.5, 117.4, 124.0, 124.1, 127.5, 133.4, 149.0, 150.0, 151.7, 157.3, 160.6, 163.6; HRMS (ESI, m/z) calcd for C₂₀H₂₄Cl₂N₇: 432.1464 (MH)⁺; Found: 432.1473; Anal. Calcd for C₂₀H₂₃Cl₂N₇: C, 55.56; H, 5.36; N, 22.68; Found: C, 55.68; H, 5.42; N, 22.73.

*N*¹-(4-chloro-6-(4-ethylpiperazin-1-yl)pyrimidin-2-yl)-*N*²-(7-

chloroquinolin-4-yl)ethane-1,2-diamine (20f): Yield: 60%; mp 116-118 °C; IR (cm⁻¹, KBr): 3310, 2969, 2853, 1576, 1489, 1447, 1140, 968, 805; ¹H NMR (400 MHz, DMSO-*d*₆): 0.95 (t, *J* = 7.3 Hz, 3 H, CH₃); 2.24-2.30 (m, 6 H, CH₂); 3.42-3.54 (m, 8 H, CH₂); 5.73 (s, 1 H, ArH); 6.49 (d, *J* = 5.1 Hz, 1 H, ArH); 7.38-7.42 (m, 3 H, NH and ArH); 7.74 (d, *J* = 2.2 Hz, 1 H, ArH); 8.12 (d, *J* = 8.7 Hz, 1 H, ArH); 8.34 (d, *J* = 5.4 Hz, 1 H, ArH); HRMS (ESI, m/z) calcd for C₂₁H₂₆Cl₂N₇: 446.1621 (MH)⁺; Found: 446.1623; Anal. Calcd for C₂₁H₂₅Cl₂N₇: C, 56.50; H, 5.65; N, 21.97; Found: C, 56.58; H, 5.81; N, 21.79.

*N*¹-(7-chloroquinolin-4-yl)-*N*³-(4-(4-methylpiperazin-1-yl)pyrimidin-2-yl)propane-1,3-diamine (20g): Yield: 54%; mp 76-78 °C; IR (cm⁻¹, KBr): 3276, 2936, 2851, 1581, 1490, 1343, 1244, 1138, 1003, 974, 794; ¹H NMR (400 MHz, CDCl₃): 2.05-2.08 (m, 2 H, CH₂); 2.30-2.39 (m, 7 H, CH₂ and CH₃); 3.44-3.55 (m, 4 H, CH₂); 3.74-3.78 (m, 4 H, CH₂); 4.86 (brs, 1 H, NH); 5.29 (brs, 1 H, NH); 5.68 (d, *J* = 5.1 Hz, 1 H, ArH); 6.38 (d, *J* = 4.4 Hz, 1 H, ArH); 7.32 (dd, *J* = 8.7 Hz, 2.2 Hz, 1 H, ArH); 7.55 (d, *J* = 8.7 Hz, 1 H, ArH); 7.88 (d, *J* = 5.1 Hz, 1 H, ArH); 7.94 (d, *J* = 2.2 Hz, 1 H, ArH); 8.49 (d, *J* = 5.1 Hz, 1 H, ArH); ¹³C NMR (100 MHz, DMSO-*d*₆): 27.6, 36.2, 37.6, 43.0, 45.8, 54.3, 98.6, 117.4, 124.00, 124.09, 127.4, 133.3, 149.0, 150.0, 151.8, 154.5, 161.2, 162.4; HRMS (ESI, m/z) calcd for C₂₁H₂₇ClN₇: 412.2010 (MH)⁺; Found: 412.2005; Anal. Calcd for C₂₁H₂₆ClN₇: C, 61.23; H, 6.36; N, 23.80; Found: C, 61.29; H, 6.19; N, 23.62.

*N*¹-(7-chloroquinolin-4-yl)-*N*³-(4-(4-ethylpiperazin-1-yl)pyrimidin-2-yl)propane-1,3-diamine (20h): Yield: 50%; mp 160-163 °C; IR (cm⁻¹, KBr): 246, 2926, 2850, 1578, 1443, 1327, 1236, 1137, 791; ¹H NMR (400 MHz, CDCl₃): 1.10 (t, *J* = 7.3 Hz, 3 H, CH₃); 2.04-2.09 (m, 4 H, CH₂); 2.39-2.43 (m, 4 H, CH₂); 3.41-3.46 (m, 2 H); 3.52-3.57 (m, 2 H, CH₂); 3.75-3.77 (m, 4 H, CH₂); 4.88 (brs, 1 H, NH); 5.26 (brs, 1 H, NH); 5.67 (d, *J* = 5.8 Hz, 1 H, ArH); 6.38 (d, *J* = 5.1 Hz, 1 H, ArH); 7.31 (dd, *J* = 9.5 Hz, 2.2 Hz, 1 H, ArH); 7.55 (d, *J* = 9.5 Hz, 1 H, ArH); 7.88 (d, *J* = 5.1 Hz, 1 H, ArH); 7.94 (d, *J* = 2.2 Hz, 1 H, ArH); 8.50 (d, *J* = 5.1 Hz, 1 H, ArH); ¹³C NMR (100 MHz, DMSO-*d*₆): 11.8, 27.2, 38.8, 43.0, 51.6, 52.1, 95.7, 98.6, 117.4, 123.9, 124.0, 127.4, 133.3, 149.0, 150.0, 151.8, 154.6, 161.1, 162.3; HRMS (ESI, m/z) calcd for C₂₂H₂₉ClN₇: 426.2167 (MH)⁺; Found: 426.2169; Anal. Calcd for C₂₂H₂₈ClN₇: C, 62.03; H, 6.63; N, 23.02; Found: C, 62.10; H, 6.71; N, 23.11.

*N*¹-(4-chloro-6-morpholinopyrimidin-2-yl)-*N*³-(7-chloroquinolin-4-yl)propane-1,3-diamine (20i): Yield: 79%; mp 230-232 °C; IR (cm⁻¹, KBr): 3397, 3326, 2927, 2859, 1579, 1491, 1447, 1247, 1111, 1073, 787; ¹H NMR (400 MHz, DMSO-*d*₆): 1.84-1.89 (m, 2 H, CH₂); 3.28-3.45 (m, 12 H, CH₂); 5.78 (s, 1 H, ArH); 6.45 (d, *J* = 5.1 Hz, 1 H, ArH); 7.32 (brs, 1 H, NH); 7.40 (brs, 1 H, NH); 7.44 (dd, *J* = 8.8 Hz, 2.2 Hz, 1 H, ArH); 7.76 (d, *J* = 2.2 Hz, 1 H, ArH); 8.25 (d, *J* = 8.7 Hz, 1 H, ArH); 8.36 (d, *J* = 5.8 Hz, 1 H, ArH); ¹³C NMR (100 MHz, DMSO-*d*₆): 27.5, 37.9, 43.6, 65.7, 92.9, 98.6, 117.4, 123.96, 123.99, 127.4, 133.3, 149.0, 149.9, 151.8, 157.1, 160.6, 163.5; HRMS (ESI, m/z) calcd for C₂₀H₂₃Cl₂N₆O: 433.1304 (MH)⁺; Found: 433.1308; Anal. Calcd for C₂₀H₂₂Cl₂N₆O: C, 55.43; H, 5.12; N, 19.39; Found: C, 55.24; H, 5.31; N, 19.44.

***N*¹-(4-chloro-6-(piperidin-1-yl)pyrimidin-2-yl)-*N*³-(7-chloroquinolin-4-yl)propane-1,3-diamine (20j)**: Yield: 72%; mp 85-87 °C; IR (cm⁻¹, KBr): 3310, 2933, 2853, 1581, 1489, 1447, 1369, 1247, 1136, 967, 786; ¹H NMR (400 MHz, DMSO-*d*₆): 1.33-1.50 (m, 6 H, CH₂); 1.85-1.88 (m, 2 H, CH₂); 3.27-3.51 (m, 8 H, CH₂), 5.69 (s, 1 H, ArH); 6.44 (d, *J* = 5.1 Hz, 1 H, ArH); 7.29-7.31 (brs, 2 H, NH); 7.42 (dd, *J* = 8.8 Hz, 2.2 Hz, 1 H, ArH); 7.75 (d, *J* = 2.2 Hz, 1 H, ArH); 8.24 (d, *J* = 8.7 Hz, 1 H, ArH), 8.35 (d, *J* = 5.4 Hz, 1 H, ArH); ¹³C NMR (100 MHz, DMSO-*d*₆): 24.2, 25.1, 27.5, 37.9, 44.0, 91.9, 98.6, 117.4, 123.9, 124.0, 127.4, 133.3, 149.0, 149.9, 151.7, 160.4, 163.4; HRMS (ESI, *m/z*) calcd for C₂₁H₂₅Cl₂N₆: 431.1512 (MH)⁺; Found: 431.1514; Anal. Calcd for C₂₁H₂₄Cl₂N₆: C, 58.47; H, 5.61; N, 19.48; Found: C, 58.51; H, 5.50; N, 19.49.

***N*¹-(4-chloro-6-(4-methylpiperazin-1-yl)pyrimidin-2-yl)-*N*³-(7-chloroquinolin-4-yl)propane-1,3-diamine (20k)**: Yield: 63%; mp 106-108 °C; IR (cm⁻¹, KBr): 3327, 2929, 1578, 1449, 1248, 1138, 1001, 785; ¹H NMR (400 MHz, DMSO-*d*₆): 1.85-1.90 (m, 2 H, CH₂); 2.06-2.16 (m, 7 H, CH₂ and CH₃); 3.41-3.47 (m, 8 H, CH₂), 5.74 (s, 1 H, ArH); 6.44 (d, *J* = 5.1 Hz, 1 H, ArH); 7.28-7.32 (brs, 2 H, NH); 7.43 (dd, *J* = 8.8 Hz, 2.2 Hz, 1 H, ArH); 7.76 (d, *J* = 2.2 Hz, 1 H, ArH); 8.25 (d, *J* = 8.7 Hz, 1 H, ArH), 8.36 (d, *J* = 5.4 Hz, 1 H, ArH); HRMS (ESI, *m/z*) calcd for C₂₁H₂₆Cl₂N₇: 446.1620 (MH)⁺; Found: 446.1621; Anal. Calcd for C₂₁H₂₅Cl₂N₇: C, 56.50; H, 5.65; N, 21.97; Found: C, 56.48; H, 5.52; N, 21.83.

***N*¹-(4-chloro-6-(4-ethylpiperazin-1-yl)pyrimidin-2-yl)-*N*³-(7-chloroquinolin-4-yl)propane-1,3-diamine (20l)**: Yield: 61%; mp 79-81 °C; IR (cm⁻¹, KBr): 3278, 2928, 1576, 1442, 1240, 1137, 1005, 785; ¹H NMR (400 MHz, DMSO-*d*₆): 0.92 (t, *J* = 7.3 Hz, 3 H, CH₃); 1.81-1.86 (m, 2 H, CH₂); 2.07-2.20 (m, 6 H, CH₂); 3.25-3.39 (m, 8 H, CH₂), 5.70 (s, 1 H, ArH); 6.41 (d, *J* = 5.1 Hz, 1 H, ArH); 7.30-7.32 (brs, 2 H, NH); 7.40 (dd, *J* = 8.8 Hz, 2.2 Hz, 1 H, ArH); 7.73 (d, *J* = 2.2 Hz, 1 H, ArH); 8.22 (d, *J* = 8.7 Hz, 1 H, ArH), 8.32 (d, *J* = 5.8 Hz, 1 H, ArH); ¹³C NMR (100 MHz, DMSO-*d*₆): 11.8, 27.6, 37.9, 43.1, 51.5, 51.9, 92.5, 98.6, 117.4, 124.01, 124.07, 127.4, 133.3, 149.0, 150.0, 151.8, 157.2, 160.5, 163.4; HRMS (ESI, *m/z*) calcd for C₂₂H₂₈Cl₂N₇: 460.1777 (MH)⁺; Found: 460.1766; Anal. Calcd for C₂₂H₂₇Cl₂N₇: C, 57.39; H, 5.91; N, 21.30; Found: C, 57.25; H, 5.95; N, 21.41.

Assay for *in-vitro* antimalarial activity

Activity was determined against both chloroquine-sensitive isolate of the human malaria parasite (*Plasmodium falciparum* Nf54) and chloroquine-resistant isolate (*P. falciparum* Dd2). Parasites were maintained in continuous culture using the method of Trager and Jensen²³ with modifications. Growth medium was supplemented with Albumax II (Gibco), a bovine serum albumin preparation, instead of human serum. Cultures did not exceed 4% haematocrit and parasitemia was diluted to 1% when the cultures were in the trophozoite stage.

The compounds were tested in triplicate on at least three occasions *in vitro* against the human malaria parasite. Compounds were prepared to 20mg/mL stock solutions in dimethyl sulfoxide and sonicated for 10 minutes to enhance solubility. Compounds which did not dissolve completely were

tested as a suspension. Stock solutions were stored at -20°C until use. For the *in vitro* evaluation, dilutions to the desired starting concentration of each compound were prepared in complete medium immediately prior to use on each occasion.

Dose-response experiments were carried out in both isolates in order to determine the IC₅₀ value of each compound. The experiment was conducted using 2% parasitemia and 1% haematocrit in the plate. Compounds were prepared to double the desired highest starting concentration in a 96-well plate and then serially diluted 2-fold in complete medium to produce a wide range of different concentrations, to which an equivalent volume of prepared parasite stock was added, yielding the desired concentration of each compound. An erythrocyte control and a drug-free parasite control were included for each row, representing 0% and 100% parasite survival respectively. Plates were housed in airtight chambers containing 4% CO₂ and 3% O₂ in nitrogen and left for 48 hours at 37 °C.

Quantitative assessment of antimalarial activity was determined from the dose-response experiments using the parasite lactate dehydrogenase assay described by Makler *et al.*²⁴ The IC₅₀-values were obtained using a non-linear dose-response curve fitting analysis via Graphpad Prism v.4.0 software.

Assay for *in-vivo* antimalarial activity

The compound was tested using the Peters 4-Day test. The parasite strain used was *Plasmodium berghei* ANKA transfected with the green fluorescent protein construct to enable detection of parasite using a flow cytometer. Mice were male Balb C (albino) mice, randomly divided into groups of five animals. Approval for the study was obtained following submission of the protocol for review by the Animal Ethics Committee at the University of Cape Town. The experiment continued until it became apparent that parasite levels were no longer suppressed and were increasing. Several days prior to the evaluation, donor mice were infected with parasites which were left to multiply to sufficiently high numbers. On the first day (Day 0) of the experiment, donor mice were killed by inhalation of excess isoflurane and their blood collected into heparinised tubes to prevent clotting. Parasitemia was determined via microscopic analysis, as was cell density. From this, blood was diluted into phosphate-buffered saline (PBS) such that each mL of the stock preparation contained 2x10⁸ parasitised erythrocytes. Mice were anaesthetised by intramuscular injection of a fixed-dose preparation of ketamine and xylazine (3:2 v/v), diluted 1:4 in phosphate-buffered saline. Each mouse was then infected with 100µL (2x10⁷) of the parasite stock intravenously. Mice were left for two hours to recover from the anaesthesia. After that, each group was dosed with either the appropriate compound or the placebo.

Compounds were dosed on Day 0 and then 24, 48 and 72 hours later. Compounds were prepared immediately prior to dosing. Chloroquine was prepared to a dose of 15mg/kg in phosphate-buffered saline and 200µL administered by gavage. The placebo group received 200µL of 0.5% (w/v) hydroxypropyl methylcellulose (HPMC) prepared in water, given by gavage. Two groups of mice received compound **30** orally, at 10mg/kg and 30mg/kg respectively. The compound was weighed out and dissolved in dimethyl sulphoxide (DMSO); the volume used was

15% of the total final volume calculated), then made up to the final volume in 0.5% HPMC as above, and sonicated for ten minutes. A final volume of 200 μ L was dosed to each animal by gavage on each occasion. For intravenous dosing the compound was prepared to 5mg/kg and dissolved in 15% of the final calculated volume in DMSO and sonicated for ten minutes. A solution of propylene glycol and ethanol (4:1 v/v) was added, comprising 40% of the total calculated volume. The balance of the volume was made up with polyethylene glycol. A total of 50 μ L was administered to each animal intravenously each day after the animals were anaesthetised as described above.

Parasite counts were determined by flow cytometry after 96 hours (Day 4) and then again on Days 7, 9 and 11, using a Becton-Dickinson FACSCalibur. On those days, a small incision was made on the tail of each animal and a small volume of blood collected into a heparinised capillary tube. The blood was expelled from the capillary into a separate tube containing 0.5mL PBS and transferred to the flow cytometer for analysis.

Molecular docking studies

The 2D structures of all the compounds were generated by drawing on ChemBioDraw Ultra 12.0 (www.cambridgesoft.com). Ligprep module implemented in Schrödinger was used to generate energy minimized 3D structures. Partial atomic charges were computed using the OPLS_2005 force field. The correct Lewis structure, tautomers and ionization states (PH 7.0 +/- 2.0) for each of these ligands were generated and optimized with default settings (Ligprep 2.5, Schrödinger, LLC, New York, NY, 2012). The 3D crystal structures of wild type PfDHFR-TS (PDB ID:3QGT; resolution 2.30 Å) and quadruple mutant (N51I+C59R+S108N+I164L) PfDHFR-TS (PDB ID:3QG2; resolution: 2.30 Å), was retrieved from protein data bank (www.rcsb.org). The proteins were prepared for docking using Protein Preparation Wizard (Maestro 10.0 Schrödinger, LLC, New York, NY, 2012). Water molecules within 5 Å of the protein structures was considered. Bond order and formal charges were assigned and hydrogen atoms were added to the crystal structure. Further to refine the structure OPLS-2005 force field parameter was used to alleviate steric clashes and the minimization was terminated when RMSD reached maximum cutoff value of 0.30 Å.

The location of co-crystallized ligand Pyremethamine in both wild and mutant protein structures were used to choose the center and size of the receptor grid, which was generated using Glide 5.8 (Schrödinger, LLC, New York, NY, 2012) with default settings for all parameters. The grid size was chosen sufficiently large to include all active site residues involved in substrate binding. The cofactor, NADH in the PfDHFR-TS wild and mutant structures were also considered as part of the receptor proteins.

All ligand conformers were docked to each of the receptor grid files (PfDHFR-TS wild and mutant structures) using Glide extra precision (XP) mode. Default settings were used for the refinement and scoring.

In silico ADMET Prediction

The pharmacokinetic profile of compounds showing good anti-malarial activity was predicted by using programs Qikprop v3.5 (Schrödinger, Inc., New York, NY, 2012). All the compounds were prepared in neutralized form for the calculation of pharmacokinetic properties by QikProp using Schrödinger's Maestro Build module and LigPrep, saved in SD format. The programs QikProp utilizes the method of Jorgensen²⁵ to compute pharmacokinetic properties and descriptors such as octanol/water partitioning coefficient, aqueous solubility, brain/blood partition coefficient, intestinal wall permeability, plasma protein binding and others.

Notes and references

- ^a Department of Chemistry, University of Delhi, Delhi-110007, India. Fax: 91-11-27667501; Tel: 91-11-27662683; E-mail: dsrawat@chemistry.du.ac.in
- ⁷⁰ [#]Current address: Chemistry Department, Deen Dayal Upadhyaya College (University of Delhi), Shivaji Marg, Karampura, New Delhi-110015.
- ^b Division of Clinical Pharmacology, Department of Medicine, University of Cape Town, Rondebosch 7700, South Africa
- ⁷⁵ [†] Electronic Supplementary Information (ESI) available: [¹H NMR, ¹³C NMR and HPLC data of selected compounds]. See DOI: 10.1039/b000000x/
- World Malaria Report 2013, WHO.
 - a) K. Hayton, R. M. Fairhurst, B. Naude, X. Z. Su and T. E. Wellems, *Front. Antimicrob. Resist.*, 2005, 401; b) C. Wongsrichanalai and C. H. Sibley, *Clin. Microbiol. Infect.*, 2013, **19**, 908
 - a) T. Mita, K. Tanabe and K. Kita, *Parasitol. Internat.*, 2009, **58**, 201; b) S. Turschner and T. Efferth, *Mini-Rev. Med. Chem.*, 2009, **9**, 206.
 - a) C. J. M. Whitty, C. Chandler, E. Ansah, T. Leslie and S. G. Staedke, *Malaria J.*, 2008, **7**, S7; b) C. J. M. Whitty and S. G. Staedke, *Clin. Infect. Dis.*, 2005, **41**, 1087; c) P. B. Bloland, M. Ettling and S. Meek, *Bull. World Health Organ.*, 2000, **78**, 1378.
 - a) A. Robert, O. Dechy-Cabaret, J. Cazelles and B. Meunier, *Acc. Chem. Res.*, 2002, **35**, 167; b) B. Meunier, *Acc. Chem. Res.*, 2008, **41**, 69; c) S. Manohar, M. Tripathi and D. S. Rawat, *Curr. Top. Med. Chem.*, 2014, **14**, 1706; d) R. Morphy and Z. Rankovic, *J. Med. Chem.*, 2005, **48**, 6523; e) F. W. Muregi, and A. Ishih, *Drug Dev. Res.*, 2010, **71**, 20; f) J. J. Walsh and A. Bell, *Curr. Pharma. Des.*, 2009, **15**, 2970.
 - V. V. Kouznetsov and A. Gomez-Barrio, *Eur. J. Med. Chem.*, 2009, **44**, 3091.
 - a) S. Manohar, S. I. Khan and D. S. Rawat, *Bioorg. Med. Chem. Lett.*, 2010, **20**, 322; b) S. Manohar, S. I. Khan and D. S. Rawat, *Chem. Biol. Drug Des.*, 2011, **78**, 124; c) S. Manohar, S. I. Khan and D. S. Rawat, *Chem. Biol. Drug Des.*, 2013, **81**, 625; d) A. Thakur, S. I. Khan and D. S. Rawat, *RSC Advances*, 2014, **4**, 20729.
 - S. Manohar, U. C. Rajesh, S. I. Khan, B. L. Tekwani and D. S. Rawat, *ACS Med. Chem. Lett.*, 2012, **3**, 555.
 - D. S. Rawat, S. Manohar and U. C. Rajesh, Indian Patent Application 661/DEL/2012.
 - K. Singh, H. Kaur, P. Smith, C. de Kock, K. Chibale and J. Balzarini, *J. Med. Chem.* 2014, **57**, 435.
 - a) D. Kumar, S. I. Khan, P. Ponnann and D. S. Rawat, *New J. Chem.*, 2014, **38**, 5087; b) S. Manohar, S. I. Khan, S. K. Kandhi, K. Raj, G. Sun, X. Yang, A. D. C. Molina, N. Ni, B. Wang and D. S. Rawat, *Bioorg. Med. Chem. Lett.*, 2013, **23**, 112; c) N. Kumar, S. I. Khan, H. Atheaya, R. Mangain and D. S. Rawat, *Eur. J. Med. Chem.*, 2011, **46**, 2816. d) N. Kumar, S. I. Khan, Beena; G. Rajalakshmi, P. Kumaradhas and Rawat, D. S., *Bioorg. Med. Chem.*, 2009, **17**, 5632; e) H. Atheaya, S. I. Khan, R. Mangain and D. S. Rawat, *Bioorg. Med. Chem. Lett.*, 2008, **18**, 1446.

12. D. J. Sullivan, H. Matile, R. G. Ridley and D. E. Goldberg, *J. Biol. Chem.*, 1998, **273**, 31103.
13. S. N. Cohen, K. O. Phifer and K. L. Yielding, *Nature*, 1964, **202**, 805.
- 5 14. a) A. Dorn, S. R. Vippagunta, H. Matile, C. Jaquet, J. L. Vennerstrom and R. G. Ridley, *Biochem. Pharmacol.*, 1998, **55**, 727; b) S. Moreau, B. Perly, C. Chachaty and C. A. Deleuze, *Biochim. Biophys. Acta*, 1985, **840**, 107.
- 10 15. A. C. de Dios, R. Tycko, L. M. B. Ursos and P. D. Roepe, *J. Phys. Chem. A*, 2003, **107**, 5821; b) A. Leed, K. DuBay, D. Sears, A. C. de Dios and P. D. Roepe, *Biochem.*, 2002, **41**, 10245.
16. D. S. Peterson, W. K. Milhous, and T. E. Wellems, *Proc. Natl. Acad. Sci. USA*, 1990, **87**, 3018.
- 15 17. J. Yuvaniyama, P. Chitnumsub, S. Kamchonwongpaisan, J. Vanichtanankul, W. Sirawaraporn, P. Taylor, M. D. Walkinshaw and Y. Yuthavong, *Nat. Struct. Biol.*, 2003, **10**, 357.
18. a) N. M. King, M. Prabu-Jeyabalan, E. A. Nalivaika and C. A. Schiffer, *Chem. Biol.*, 2004, **11**, 1333; b) K. P. Romano, A. Ali, W. E. Royer and C. A. Schiffer, *Proc. Natl. Acad. Sci. USA*, 2010, **107**, 20986.
- 20 19. QikProp User Manual Copyright © 2013 Schrödinger, LLC.
20. J. J. Lu, K. Crimin, J. T. Goodwin, P. Crivori, C. Orrenius, L. Xing, P. J. Tandler, T. J. Vidmar, B. M. Amore, A. G. E. Wilson, P. F. W. Stouten and P. S. Burton, *J. Med. Chem.*, 2004, **47**, 6104.
- 25 21. P. Artursson, K. Palm and K. Luthman, *Adv. Drug. Deliv. Rev.*, 2001, **46**, 27.
22. M. V. N. de Souza, K. C. Pais, C. R. Kaiser, M. A. Peralta, M. L. Ferreira and M. C. S. Lourenco, *Bioorg. Med. Chem.*, 2009, **17**, 1474.
23. W. Trager and J. B. Jensen, *Science*, 1976, **193**, 673.
- 30 24. M. T. Makler, J. M. Ries, J. A. Williams, J. E. Bancroft, R. C. Piper, B. L. Gibbins and D. J. Hinrichs, *Am. Soc. Trop. Med. Hyg.*, 1993, **48**, 739.
25. E. M. Duffy and W. L. Jorgensen, *J. Am. Chem. Soc.*, 2000, **122**, 2878.